

Surviving companions of Type Ia supernovae: theory and observations

Pilar Ruiz-Lapuente^{1,2}

Received _____; accepted _____

¹Instituto de Física Fundamental, Consejo Superior de Investigaciones Científicas, c/. Serrano 121, E-28006, Madrid, Spain

²Institut de Ciències del Cosmos (UB-IEEC), c/. Martí i Franques 1, E-08028 Barcelona, Spain

ABSTRACT

We review the theoretical background and the observational searches made for surviving companions of Type Ia supernovae (SNe Ia). Theory comprises the characteristics of the stellar binary companions of the exploding white dwarfs at the time of the supernova outburst and the expected effects on them of the explosion, as well as their subsequent evolution. That includes space velocities, rotation, luminosities (with discussion of possible mechanisms producing very faint companions) .

We then present the searches already made in the Galactic remnants of Type Ia supernovae and we assess the results obtained up to now using ground-based telescopes and the *Hubble Space Telescope* (*HST*). The same is done for the remnants of this type in the Large Magellanic Cloud. We point to new SNRs of Type Ia that can be studied with groundbased telescopes, the *HST* and the *James Webb Space Telescope* (*JWST*), using various approaches such as characterization of peculiar stars through color-magnitude diagrams, determination of their stellar parameters by spectral fitting, and astrometric measurements. *Gaia* can provide, as well, useful astrometric information. Most of these approaches have been used in the SNe Ia remnants already explored. The future goal is to enlarge the sample to determine which stellar systems do actually produce these explosions.

Subject headings: Supernovae, general; supernovae, Type Ia; supernova remnants

1. Introduction

Type Ia supernovae (SNe Ia) are distance indicators that have made possible the discovery of the accelerated expansion of the Universe (Riess et al. 1998; Perlmutter et al. 1999) and continue to be powerful probes for investigating the nature of dark energy. SNe Ia arise as thermonuclear explosions of white dwarfs (WDs) in close binary systems, brought about by mass gain of the WDs from their companion star. The nature of that companion star can either be a main sequence, subgiant, red giant, AGB, He star or another WD. The mode of mass gain can be through Roche-lobe overflow, stellar wind, merging or collision with a companion WD, merging with the electron-degenerate core of a red giant. That bears also on the way explosive thermonuclear burning is ignited and how it propagates inside the WD.

A scenario (single degenerate scenario or SD) is that in which a WD grows close to the Chandrasekhar mass by accretion from a companion star and ignites when the central density reaches $\rho > 10^9$ (Whelan & Iben 1973; Nomoto 1982). The companion will survive in this case. The alternative is the double-degenerate scenario (DD) which involves the merger of two electron degenerate objects, either two WDs (Webbink 1984; Iben & Tutukov 1984) or a WD and the core of an asymptotic giant branch (AGB) star (Livio & Riess 2003; Soker 2013; 2014; 2019). In this case there is no surviving companion.

A number of reviews have dealt with the progenitors of Type Ia SNe (Wang & Han 2012; Livio 2013; Maoz. Mannucci & Nelemans 2014; Ruiz-Lapuente 2014) and their explosion mechanisms (Hillebrandt & Niemeyer 2000; Hillebrandt et al. 2013).

The bulk of the SNe Ia is best explained by the explosive ignition of a CO mixture, close to the center of a WD with a mass near to the Chandrasekhar mass. That is supported by many observations (Nomoto & Leung 2017). The thermonuclear burning

would propagate subsonically at first (deflagration) and make a transition to the supersonic regime (detonation), when reaching layers at lower densities.

Models involving CO WDs with masses below the Chandrasekhar mass have also been proposed (see the review of Hillebrandt et al. 2013). The most viable mechanism, in this case, would be accretion of He on the surface of the WD, followed by its detonation. Compression of the CO core would, in turn, induce its detonation (Fink et al. 2010). It is not clear that this mechanism could fit the observed characteristics of most SNe Ia (Sim et al. 2012).

Recently, observations of MUSSES1604D (Jiang et al. 2017) have lend some support to the double detonation scenario, for a particular subtype of SNe Ia. The spectrum of an early red flash seems to be best explained by explosive thermonuclear burning close to the surface of the WD. A He WD might have been the mass donor and there is even the possibility that it survived the SN explosion (Shen & Schwab 2017; Shen et al. 2018).

Here, we specifically address the direct searches for surviving companions of SNe Ia in SN remnants and their theoretical background. In that, the information about the remnants is crucial for developing the search of possible companions.

Having said that, we know about 300 SN remnants in our Galaxy (Green 2014), but their classification as SN Ia remnant or as Core Collapse (CC) SN remnant is based on the characteristics of their X-ray spectra. There are a couple of tens of SNRs classified unambiguously as SN Ia or CC SN. This type of classification has been made as well for a number of SNRs in the Large Magellanic Cloud. Four SNe Ia correspond to well known observed events in our Galaxy: SN 1604 (known as Kepler’s SN), SN 1572 (Tycho’s SN), SN 1006, and SN 185 (thought to correspond to the SNR RCW 86). The SN 1885A, in the Andromeda galaxy, has also been classified as SN Ia and its remnant located and studied.

Detailed searches for companions in SNe Ia remnants were only conducted after 1997. Specifically, data were collected to look for peculiar velocities, excess luminosities, spectroscopic and chemical anomalies in the stars located in the central regions of recently produced, nearby SNRs of the Ia type. These searches were performed in order to either identify such companions or discard their presence (early work by Ruiz-Lapuente 1997; Ruiz-Lapuente et al 2004). Tycho’s SNR was first to be explored and to be subsequently investigated in a number of papers (Ruiz-Lapuente et al. 2004; Ihara et al. 2007; González Hernández et al. 2009; Kerzendorf et al. 2009, 2013, 2018a; Bedin et al. 2014; Ruiz-Lapuente et al. 2019). The remnants of SN 1006 (González Hernández et al. 2012; Kerzendorf et al. 2012, 2018b) and of Kepler’s SN (Kerzendorf et al. 2014; Ruiz-Lapuente et al. 2018) have followed. In the LMC, five SNRs have been explored to some extent (Schaefer & Pagnotta 2012; Edwards, Pagnotta & Schaefer 2012; Pagnotta & Schaefer 2015; Li et al. 2017, 2019).

This paper is organized as follows: In Section 2, we first review our theoretical knowledge of the physical features that should or might characterize the surviving companions of SNe Ia (including some progenitor evolution scenarios that result in unusual survivors). In section 3, we describe the work that has been done up to now exploring the Galactic SNRs attributed to SNe Ia. We also discuss what has been achieved on the SNRs in the LMC. The last Section summarizes what we have learned thus far about the SNe Ia companions.

2. Theoretical predictions for surviving companions

There are three main areas for exploring the nature of surviving companions of SNe Ia: 1) evolution up to the explosion of the WD; 2) interaction of the ejecta with the WD, and 3) the (long-term) post-impact evolution of the companion.

The first and the last one lie in the realm of (binary) stellar evolution codes while the second one is mostly explored using hydrodynamical simulations.

There have been several studies in the last decade that explore some parts of the parameter space of the whole process from co-evolution of the binary system to the final fate of the companion.

2.1. Luminosities of possible surviving companion stars

There have been analytical studies of the impact of a supernova explosion on a binary companion (Wheeler, McKee & Lecar 1974; Wheeler, Lecar & McKee 1975), using a polytropic model for the companion star and a plane-parallel approximation for the structure of the supernova ejecta.

The first detailed hydrodynamical (2D) simulations of the impact of SN Ia ejecta on a companion star, considering companions of different types (main sequence, subgiant, red giant), and estimating the post-impact luminosities, have been those of Marietta, Burrows & Fryxell (2000). They have been followed by those of Pakmor et al. (2008) (3D; main sequence companion (MS) only), of Pan, Ricker & Taam (2012a,b; 2014) (2D and 3D; main sequence, red giant (RG) and He star companions), and of Liu et al. (2013) (3D; main sequence companion).

The post-impact evolution of the companion star can only be followed at most up to the time when quasi-hydrostatic equilibrium is restored (on the order of hours to days) due to the limitations of hydrodynamical simulations. The star is then still far from thermal equilibrium. However, potential companion candidates, found in nearby SNe Ia remnants, are several hundred years old (the youngest of which, Kepler SNR, is now more than 400 years old).

In order to compare the hydrodynamical simulations of the impact on a companion star with observations, a stellar evolution code has to be used to cover the time interval between explosion and observations. Marietta, Burrows & Fryxell (2000) mostly speculated about the long-term evolution of the companion.

According to Marietta, Burrows & Fryxell (2000), main sequence companions, while out of thermal equilibrium, might reach a luminosity of 500–5,000 L_{\odot} , with a cooling timescale of 1,100–1,400 yr. After thermal equilibrium is reestablished, they would return to the main sequence more slowly, and continue the evolution corresponding to their mass (now reduced by the interaction with the SN ejecta). Subgiants would have a similar evolution, returning in a long term to a post-main-sequence track with a slightly lower luminosity than before impact.

In the red giant case, the degenerate core is left surrounded by a hot, H/He atmosphere. The residual envelope, with a small mass, when settling back down to a thin layer, might reignite H shell burning. The star should evolve away from the red giant branch, along a track of constant luminosity and increasing effective temperature, on a timescale of 10^5 – 10^6 yr. Marietta, Burrows & Fryxell (2000) emphasize that the post-impact evolution should be handled with a 2D code, able to deal with initial models that are asymmetric in density and temperature and out of thermal equilibrium.

The long-term evolution of the companion star has been first calculated by Podsiadlowski (2003), for the subgiant case. It is a 1D calculation. To construct the initial model, mass is removed at a very high rate from a subgiant model in quasi-hydrostatic and thermal equilibria. A uniform heating source is then added to the remaining outer layers, and the subsequent re-equilibration of the star is followed. In this treatment of the problem, the energy injected by the impact is deposited uniformly in the outermost 90% radial extent of the star. The amount of that energy is a free parameter, and depending from its amount

very different results are obtained: a few centuries after the explosion the companion might appear from overluminous to underluminous, as compared with the pre-impact model. An important result is that the re-equilibration of the outermost layers is much faster than the thermal timescale (i.e. the time to reach thermal equilibrium) of the whole envelope of the initial subgiant.

More recently, Shappee, Kochanek & Stanek (2013) have explored the evolution of a main sequence companion of $1 M_{\odot}$. They use the stellar evolution MESA (Modules for Experiments in Stellar Astrophysics) code (Paxton et al 2011) (1D) code.³ They first simulate the stripping of mass from the star by an initial phase of rapid mass loss, but then they introduce a second phase when they add a heating source, which induces a wind that would simulate the mass loss by ablation (as in Podsiadlowski 2003). The internal energy added per unit mass is made proportional to the ratio of the enclosed mass at a given radius to the total mass of the model. Then they follow the subsequent evolution and find that the star should remain overluminous (10 to 1,000 L_{\odot}) for 1,000 to 10,000 yr.

The most recent calculation of the post-impact evolution is that of Pan, Ricker & Taam (2012b). They use again the 1D MESA code, but starting from the results of their own hydrodynamic simulations (Pan, Ricker & Taam 2012a). The time steps are made very short initially, to closely follow the evolution when the star is still very far from equilibrium. They find that the evolution of the star not only depends on the amount of energy absorbed in the impact but also on the depth of the energy deposition. They suggest that shock compression is an important factor (which has been ignored in some other studies) and they criticize the arbitrary setting of the depth of energy deposition in previous work.

The post-impact companion stars rapidly expand on time scales $\sim 10^2 - 10^3$ yr (depending

³<http://mesa.sourceforge.net>

Table 1: The models in Pan, Ricker & Taam (2012b). (Courtesy of Kuo-Chuan Pan. @AAS. Reproduced with permission.)

Model	M_i	P_i	R_i	L_i	$T_{eff,i}$	M_f	P_f	R_f	L_f	$T_{eff,f}$
	(M_\odot)	(day)	(R_\odot)	(L_\odot)	(K)	(M_\odot)	(day)	(R_\odot)	(L_{odot})	(K)
A	2.51	0.477	1.83	39.2	10696	1.88	0.350	1.25	2.35	6392
B	2.51	0.600	2.08	42.4	10224	1.92	0.466	1.50	3.64	6516
C	3.01	1.23	3.64	110.0	9800	1.82	1.09	2.63	8.06	6003
D	2.09	0.472	1.67	19.2	9358	1.63	0.353	1.19	2.09	6372
E	2.09	0.589	1.91	20.8	8933	1.59	0.470	1.42	3.15	6450
F	2.09	0.936	2.59	23.9	7934	1.55	0.770	1.97	5.09	6182
G	2.00	1.00	1.70	17.6	9083	1.17	0.233	0.792	0.463	5355

The mass (M_i), period (day), radius (R_i), luminosity (L_i), and effective temperature ($T_{\text{eff},i}$) for different companion models at the beginning of RLOF for WD+MS systems, using the initial masses and orbital periods in Figure 7 of Hachisu, Kato & Nomoto (2008), are given in columns 2–6. The mass (M_f), period (day), radius (R_f), luminosity (L_f), and effective temperature ($T_{\text{eff},f}$) for companion progenitor models at the time of the SN explosion. See Figure 1.

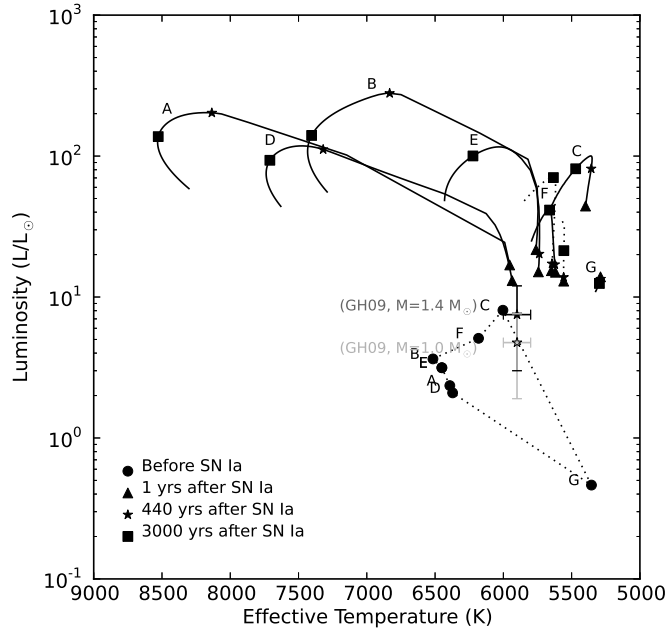


Fig. 1.— Evolutionary tracks in the H–R diagram, for the different post–impact companion models in Table 1. Each track corresponds to the evolution for 10^4 yr of one of these models. Filled circles mark the conditions of the stars just before the SN explosion. Filled triangles, those ~ 1 yr after explosion. Star symbols, 440 yr after it (the age of Tycho’s SN). Filled squares, 3000 yr after explosion. The star symbol with error bars shows the observed luminosity and effective temperature of star G as measured by González Hernández et al. (2009). Pan, Ricker & Taam (2012b). (Courtesy of Kuo-Chuan Pan. ©AAS. Reproduced with permission.)

on the pre-impact structure). Initially, the luminosity inside the envelope is much higher than the surface luminosity. Due to that, the outermost $\lesssim 1\%$ of mass expands and the luminosity profile in the outermost 10% of mass flattens due to radiative diffusion. The local thermal time scale in the envelope region is much shorter than the global thermal time scale. After ~ 200 yr, the deposited energy has been radiated away and the star begins to contract, releasing gravitational energy. The luminosity decreases and the effective temperature increases. It will return to the Zero-Age Main Sequence (*ZAMS*) on a global thermal time scale. The luminosities, 440 yr after the explosion (Figure 1), could be as low as $\approx 13 L_{\odot}$, which is far below the predictions of Shappee, Kochanek & Stanek (2012). Interestingly, all models considered by Pan, Ricker & Taam (2012b) have, at the referred time, effective temperatures $T_{\text{eff}} \gtrsim 5300$ K. In a later work, Pan, Ricker & Taam (2014) present in more detail the observable characteristics of post-impacted MS and He WD companions, such as their color and luminosity evolution. It is worth noticing that their new class of companion models, the He WDs, as they were in a closer orbit with the exploding WD, gained higher velocities and reached effective temperatures on the range of T_{eff} from 10,000K to 70,000 K.

2.2. Ejection velocities

Typically, the SNe Ia explosion will disrupt the binary system (in non-merging systems). The companion, its linear momentum unchanged, will start moving along a straight line, with the orbital velocity it had at the time of the explosion. The SN ejecta, moving much faster, will overrun it and the portion intercepted by the companion will impart a kick, strip some mass from its outer layers, and inject some energy into the material that remains bound (the latter inducing extra mass ejection and puffing up). The escape velocity and kick might give the companion an unusual kinematic signature when compared with the

surrounding stars. Hydrodynamical simulations (Marietta, Burrows & Fryxell 2000) of the interaction between ejecta and companion showed that the kinematic effect of the kick (imparted perpendicularly to the orbital velocity) was minor as compared with the escape velocity. The momentum gained from the kick depended on orbital separation and on how compact the companion was. It ranged from 12% to 50% of the momentum the star had before the explosion in the cases of main-sequence and subgiant companions, the kick being much smaller in the case of red giants. Similar values have later been found by Pan, Ricker & Taam (2014).

The orbital velocities depend on the nature of the companion star of the WD. Since the companion is assumed to be filling its Roche lobe at the time of the explosion (save in the case of wind-accretion systems, where the WD accretes matter from the wind of a red-giant or supergiant star), the orbital separation a should be smallest for main-sequence companions and largest for red-giant ones. Using Eggleton’s (1983) approximation for the radii of the Roche lobes:

$$R_L = a \left[\frac{0.49}{0.6 + q^{-2/3} \ln(1 + q^{1/3})} \right] \quad (1)$$

where R_L is the Roche-lobe radius of the secondary star and $q \equiv M_2/M_1$; we see that for a fixed q , in order for the secondary to be filling its Roche lobe the separation has to vary as the radius of the star. Then, assuming circular orbits, we have from Kepler’s law that

$$P^2 = \frac{a^3}{M_1 + M_2} \quad (2)$$

where P is the period in years of the binary, a the orbital separation in astronomical units, and M_1 , M_2 are in solar masses. So we have that $v_{\text{orb}} \propto a^{-1/2}$, and the main-sequence companions should move faster than the red-giant ones. If we look at the typical velocities

for main–sequence stars, subgiants and red giants obtained by Marietta, Burrows & Fryxell (2000) and Han (2008), those are of 250–300 km s^{−1}, 150 km s^{−1}, and 80 km s^{−1} respectively.

There is also the possibility, within the double–degenerate channel to produce SNe Ia, that the explosion could be triggered just at the beginning of the coalescence process of the two WDs, by detonation of a thin helium layer coming from the surface of the less massive object, which would then compress the more massive WD and detonate its core (Shen et al. 2018). The less massive WD would thus survive. In that case, the orbital velocity being very high (> 1000 km s^{−1}), a hypervelocity WD would be ejected. Shen et al. (2018) claim that three objects found in the DR2 from the *Gaia* space mission are in fact such hypervelocity WDs. They do not look as typical WDs but they might result from heating and bloating of a WD companion. WDs with $M \gtrsim 0.15 M_{\odot}$, however, do not become significantly bloated when heated. That can be seen from the WD cooling curves, since the heating due to the impact of the supernova ejecta should follow the same curves, now towards increasing temperatures. Only very low mass WDs are the outcome of stars resembling those hypervelocity objects.

Since, in general, the peculiar velocity of a surviving companion will form any angle with the line of sight to the SNR, it should be detected as both an excess in radial velocity and in proper motion, as compared with the average of the stars at the same location within the Galaxy (or the host galaxy, in the case of extragalactic SNe Ia). A common problem when examining possible candidates to SNe Ia companions is to determine their distances. Accurate distances to individual stars have to be obtained, most of the time, by deducing their spectral types and luminosity classes from their spectra and then comparing the absolute magnitudes in different passbands with photometric measurements. The same spectra are used to measure the radial velocities. Concerning proper motions, astrometric

measurements from *Hubble Space Telescope* images taken at different epochs have been used.

2.3. Rotation

In close binary systems, tidal interaction tends to make rotation of the component stars synchronous, that is, to make the rotation period equal to the orbital period. The gravitational attraction of the companion star induces a tidal bulge on each component of the system (the same way as the Moon acts on the Earth’s oceans). Synchronization is due to the viscosity of the fluid the star is made of.

When rotation is not synchronous, the tidal bulge creates a torque that either accelerates rotation when its period is longer than the orbital period or slows it down when it is shorter.

The timescale for synchronization, for a given initial system and any other influences on rotation (such as mass loss) being absent, thus only depends on the viscosity of the fluid: the higher the viscosity, the shorter the timescale. When the envelope of the star is in radiative equilibrium, only radiative damping acts and the timescales are long. When the envelope is convective, turbulent viscosity, much higher, is the relevant one and the timescales are much shorter.

Main sequence companions with masses $M \lesssim 1.3 M_{\odot}$, subgiants, and red giants do possess surface convection zones. Therefore, we should expect that, in systems made of a white dwarf plus a companion of one of these types, from tidal interaction alone, and for times like those mediating between the epoch when the system becomes close and that of the SN Ia explosion, the rotation had become synchronous.

We are ignoring here the loss of angular momentum due to mass loss (mass transferred

to the white dwarf plus mass lost by the system) by the companion star, which should slow the rotation down. For fast mass losses, that would compete with the synchronization mechanism.

The rotation of the companion star post-explosion is likely not that of pre-explosion but smaller, due to several effects. From all the existing hydrodynamic simulations, mass is reduced by stripping (momentum imparted) and ablation (energy deposition that unbinds layers that are below those removed by stripping). For a given total amount of mass lost, matter that was at some depth inside the star then becomes the new surface layer.

In all simulations, immediately after the explosion main sequence stars and subgiants do not just recover their former radii but are puffed up and do not return to the radii corresponding to their new masses and to their evolutionary stages until thermal equilibrium is restored (between 1400 and 11000 yr, in Marietta, Burrows & Fryxell 2000). Red giants lose almost all their envelope and the residual one also expands. When it recontracts, H shell burning, temporarily extinguished, could be reignited and the star recover its former luminosity with a smaller radius (Marietta, Burrows & Fryxell 2000), although this is still mostly speculation by now. During this contraction phase the star would spin up.

Liu et al. (2013) have made 3D Smoothed Particle Hydrodynamics (SPH) simulations of the impact of SN Ia ejecta on a main-sequence companion of $1 M_{\odot}$, using the GADGET-3 code (Springel et al. 2001; Springel 2005). The evolution of the binary system previous to the explosion has been calculated with a 1D stellar evolution code (Eggleton 1973). Figure 2 displays the evolution in luminosity of the donor star and Figure 3 that of the orbital velocity.

In these simulations the rotational velocity of the companion star is significantly reduced to about 14% to 32% of its pre-explosion value due to the expansion of the companion

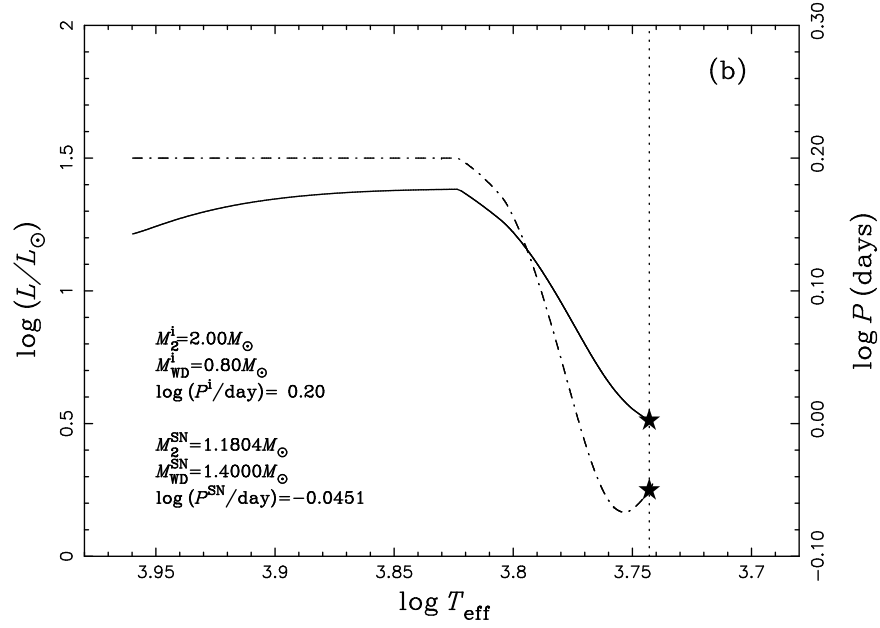


Fig. 2.— Evolution of the luminosity (left vertical axis) and the orbital period (right vertical axis) of the donor star and of the system, respectively, in one of the models calculated by Liu et al. (2013), up to the point of explosion. The solid curve corresponds to the evolution of the donor and the dash-dotted curve to that of the period. (Courtesy of Zhen-Wei Liu. ©Springer A & A. Reproduced with permission.)

and because 35% to 89% of the initial angular momentum is carried away by the stripped matter (see Figure 3). Liu et al. (2013) also find that the radial distribution of the rotation of the companion becomes approximately constant $\sim 10^4$ s after the explosion (Figure 3).

Table 2: The impact simulations of Liu et al. (2013). (Courtesy of Zhen-Wei Liu. @Springer A & A. Reproduced with permission.)

Model	M_2^{SN}	P^{SN}	R_2^{SN}	a^{SN}	v_{rot}^{SN}	v_{rot}^f	v_{rot}^{ff}	J_{spin}^{SN}	J_{spin}^f	M_{bound}
	$[M_\odot]$	[days]	$[R_\odot]$	$[R_\odot]$		$[\text{km s}^{-1}]$		$[10^{50} \text{ g cm}^2 \text{ s}^{-1}]$		$[M_\odot]$
MS-160	1.21	0.29	0.93	2.55	160	52	98	2.94	1.31	1.04
MS-131	1.23	0.56	1.45	3.94	131	40	78	2.07	0.92	1.06
MS-110	1.18	0.91	1.97	5.39	110	25	46	2.25	0.62	0.95
MS-081	1.09	2.00	3.19	8.92	81	12	16	2.32	0.26	0.84

Here, M_2^{SN} , P^{SN} , R_2^{SN} , a^{SN} , v_{rot}^{SN} and J_{spin}^{SN} are the mass, the orbital period, the radius, the spin velocity and angular momentum of the companion star at the moment of the explosion, respectively. v_{rot}^f , J_{spin}^f and M_{bound} denote the spin velocity, the angular momentum, and the total bound mass of the companion star after the SN impact. v_{rot}^{ff} is the rotational velocity at the surface after the thermal equilibrium is reestablished. Note that the rotational velocity, v_{rot}^{SN} , is calculated by assuming that the rotation of the star is locked with the orbital motion due to tidal interactions. These four models are shown in Figure 3.

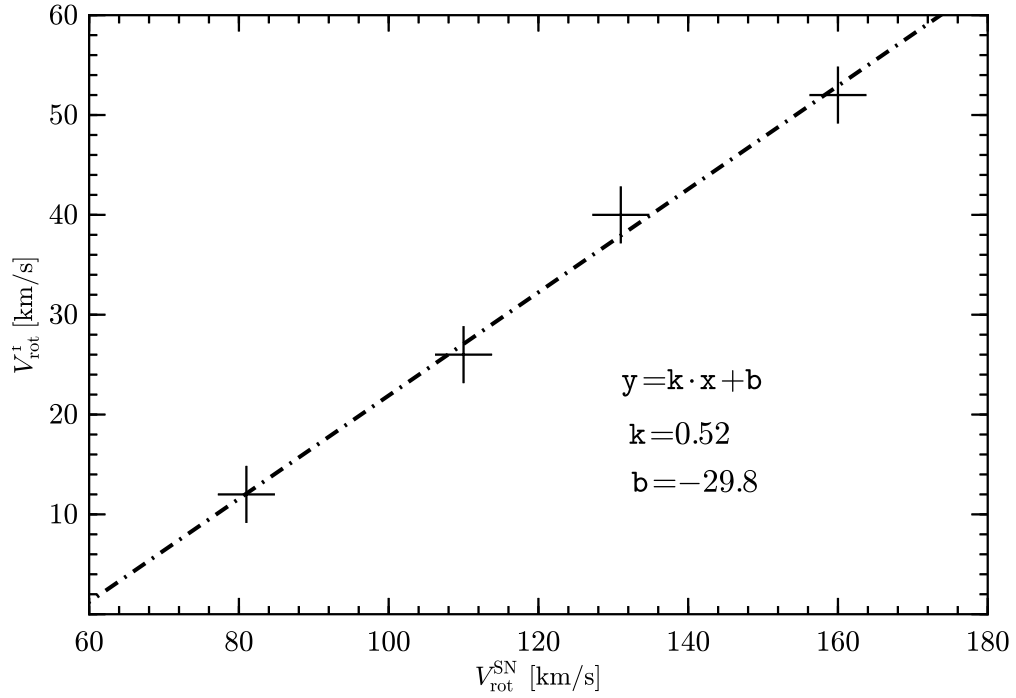


Fig. 3.— Initial rotational velocity at the time of the SN explosion *vs.* rotational velocity after the explosion, for four different models from Liu et al. (2013). The crosses correspond to the four models of Table 2. (Courtesy of Zhen-Wei Liu. @Springer A & A. Reproduced with permission.)

Pan, Ricker & Taam (2012a,b; 2014) have made 3D hydrodynamic simulations of SN impacts on different companion models, using the FLASH version 3 code (Fryxell et al. 2000; Dubey et al. 2008). The progenitor systems were constructed and the post-impact evolution of the remnant star followed with MESA. The progenitor models were taken from Hachisu, Kato & Nomoto (2008), who studied the binary evolution of WD+MS systems and found the region of the donor mass–orbital period plane where SNe Ia can occur, but they were recalculated with the MESA code from the ZAMS to the Roche-lobe overflow. Most companion stars of the WD are slightly evolved MS stars at the time of the explosion, but some of them were still close to the ZAMS. Their masses ranged between 2 and $3M_{\odot}$.

From the hydrodynamic simulations, the companion stars are heated and lose $\sim 10\%$ – 20% of their mass due to stripping and ablation by the SN ejecta. To follow the subsequent evolution, the resulting 3D models are turned into 1D models. The specific angular momentum is that obtained from the 3D simulations.

Figure 4 shows the evolution of the surface rotational speed for all the remnant star models considered by Pan, Ricker & Taam (2012b). We see that, after the impact, the rotation speed decreases as the post-impact remnant star is expanding. In the most rapidly evolving models (stars A, B, and D), the rotation speed falls to less than 10 km s^{-1} within the first 500 yr. Past 1000–1500 yr, the stars start to contract slowly, increasing the surface rotation speed. Therefore, according to these calculations, the post-impact remnant stars do not need to be fast rotators even in the WD plus main-sequence systems.

2.4. The spin-up/spin-down mechanism

In the “classical” SD channel (Whelan & Iben 1973; see Introduction), accretion makes the mass of the WD grow until reaching the Chandrasekhar mass, M_{Ch} , at which point the star

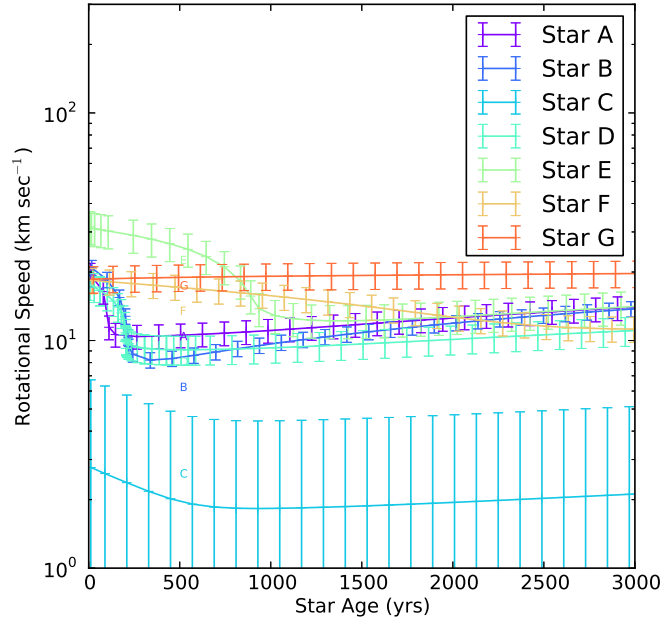


Fig. 4.— Evolution of surface rotational speed for different companion models considered by Pan, Ricker & Taam (2012b) (see Table 1). (Courtesy of Kuo-Chuan Pan. @AAS. Reproduced with permission.).

begins to contract fast and explosive C burning is ignited at its center (or close to it). In that case, to the mass growth also corresponds gain of angular momentum by the WD. That would be the spin-up stage in the evolution of the binary system.

In a rotating WD, the critical mass, M_{crit} , can considerably exceed M_{Ch} . Ostriker & Bodenheimer (1968) found, for an extreme case of differential rotation, that a mass as high as $4M_{\odot}$ would still be stable, while Yoon & Langer (2004, 2005) calculated that WDs could reach $\approx 2M_{\odot}$ before exploding.

Assuming that mass transfer stops at some point, due to exhaustion or contraction of the companion’s envelope, before the absolute stability limit for the WD is reached, one would be left with a detached binary made of a rotating, super-Chandrasekhar mass WD plus an evolving companion. Then, rotation might start to slow down, until the point is reached where the decreasing M_{crit} becomes equal to the actual mass of the WD. That would be the spin-down stage.

Faint white dwarf companions:

During the spin-down stage, the companion star of the WD continues to evolve and it could lose all its envelope (if it had not lost it at the end of the spin-up stage already), its core becoming electron-degenerate and the star, then a second WD, starting to cool down and be ever dimmer. That is the original spin-up/spin-down mechanism (Di Stefano, Voss & Claeys 2011; see Figure 5).

If the spin-down stage lasted long enough, at the time of the SN explosion the ejected, surviving companion could be dim enough to escape detection in the searches made up to now in the central regions of the remnants of SNe Ia. It would also explain (Justham 2011) the absence of H lines in the nebular spectra of SN Ia (Leonard 2007).

There are several unknowns affecting the explicative power of the spin-up/spin-down

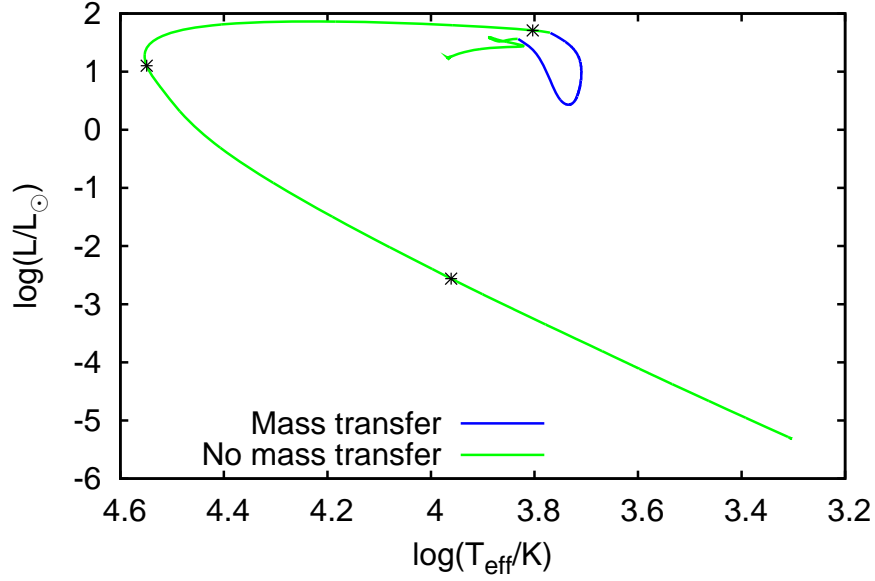


Fig. 5.— Hertzsprung–Russell diagram of the donor star in an initial binary system of a $0.7M_{\odot}$ WD and a $2M_{\odot}$ MS star and initial orbital period of 2.4 days. Blue indicates the phase of mass transfer onto the WD. The mass accretion rate is based on Hachisu et al. (1996, 1999). Mass transfer starts when the donor star is in the Hertzsprung gap and continues on the GB. After mass transfer the donor evolves into a He WD. The final system is a WD of $\sim 1.5 M_{\odot}$ and a companion of $\sim 0.3 M_{\odot}$. The crosses indicate different times after mass transfer has ceased (10^6 , 10^7 , and 10^9 years). After 10^6 yr: the donor will appear as a low-mass He–star, 10^7 yr: as a hot He WD, and 10^9 yr: as a cooler He WD. Di Stefano, Voss & Claeys (2011). (Courtesy of Rosanne Di Stefano @AAS. Reproduced with permission.)

mechanism. A first one, pointed out by Meng & Podsiadlowski (2013) is whether a WD can actually gain significant angular momentum by accretion of material from its companion. Based on the evidence gathered from fast-spinning WDs in close binary systems, it may seem that a strong magnetic field were necessary for spin-up, not just gas friction.

Even if the WD is spun-up significantly, solid-body rotation only slightly increases M_{crit} above M_{Ch} (Yoon & Langer 2004, 2005). Only differential rotation can make WDs with masses up to $\approx 2 M_{\odot}$, and even higher, stable. Therefore, the spin-down time scale is set by that of the redistribution of angular momentum inside the WD, approaching solid-body rotation. Such time scale is very uncertain (and also the distribution of angular momentum at the start of spin-down): Yoon & Langer (2005) find an upper limit of $\sim 10^6$ yr only. Acknowledging the difficulty of a theoretical determination, Meng & Podsiadlowski (2013) adopt a semi-empirical approach: assuming the companion to be a red giant at the end of spin-up, and based on the presence of circumstellar material coming from the envelope of the companion, in some SNe Ia at least, they set an upper limit of $\sim 10^7$ yr to the spin-down time scale. It is, therefore, unclear that the companion stars could be dim enough, at the time of the SN explosion, to easily escape detection.

A possible objection to the spin-up/spin-down mechanism is that the bulk of the SNe Ia are not super-Chandrasekhar: the Galactic SNe Ia whose light curves have been reconstructed (Ruiz-Lapuente 2004, 2017) appear to be completely “normal”. Since there is nothing to make the spin-up stop when the WD reaches the Chandrasekhar mass, it may seem that the super-Chandrasekhar SNe Ia should then be more common. But only, as noted above, differential rotation can support WDs with masses significantly higher than the Chandrasekhar mass. If the WD rotates almost as a solid body, the only slightly super-Chandrasekhar mass would not have a noticeable effect in the SNe Ia observable characteristics. That would also explain why there is not a wide span of masses of WDs

above the Chandrasekhar mass that explode as SNe Ia.

A further point is that nobody has yet calculated the effects that the impact of the SN ejecta would have on a WD companion, however dim it were before, save in the case of extremely close ones, ejected when they were starting to merge with the WD that explodes (Shen & Schwab 2017).

Subdwarf B star companions:

Based on the common-envelope wind model for SN Ia (Meng & Podsiadlowski 2017), Meng & Li (2019) have very recently presented new evolutionary calculations for binaries initially made of a WD plus a main-sequence companion. They find that, including the spin-up/spin-down mechanism, the companion, at the time of the SN explosion, could either be a main-sequence star, a red giant, or a subdwarf B (sdB) star, that assuming that the spin-down time scale were $\lesssim 10^7$ yr (the upper limit derived in Meng & Podsiadlowski 2013).

In the common-envelope wind model, there is no merging of the WD with its companion, the SN Ia taking place either in the common-envelope phase, in a phase of stable H burning, or in a weakly unstable phase of H burning. The companion type when the SN occurs depends on the initial parameters of the system, the sdB type generally corresponding to the highest mass ratios $q \equiv M_2/M_1$. The effective temperatures and luminosities of the sdB companions, at explosion, are in the range 30000 – 40000 K and $10L_\odot - 65L_\odot$, respectively. Meng & Li (2019) estimate that $\approx 22\%$ of the initial WD + main-sequence star systems should end up as WD + sdB. Given the typical T_{eff} of these companions, they should be searched, preferentially, in the U or UV bands.

3. Remnants of Type Ia supernovae for the exploration of surviving companions

3.1. Strategy of the searches

The search for possible surviving companion stars of SNe Ia in SNRs previously identified as produced by SNe of this type, starts with the determination of the site of the explosion and of its uncertainty. A first approximation is the geometrical centroid of the SNR. If the ejection of material was spherically symmetric and the circumstellar and interstellar media homogeneous around the location of the SN, the edge of the SNR, projected on the sky, should appear circular and the approximation would be accurate. However, even in almost circular SNRs, some degree of asymmetry exists. By that reason alone, the region to be explored must cover, even in those cases, a significant fraction of the radius of the SNR.

Even if the explosion site were very accurately known, the companion must have left the binary system with the orbital velocity it had at the time of the explosion, plus the kick imparted by the collision with the SN ejecta. That should translate into proper motion (in any direction), so the star will be found at some angular distance from the explosion site. The highest velocities expected, for still thermonuclearly evolving companions, are for main-sequence stars, and they are adopted to estimate the maximum angular distance to be covered, that depending, of course, on the age of the SNR. Possible surviving WD companions could move much faster and the area to be covered when searching for them increases accordingly (Kerzendorf et al. 2018b).

The stars to be analyzed must not only be inside some area in the sky (size dependent on the above considerations), but also at distances compatible with that of the SNR. The latter are not very accurately known in the case of most Galactic SNRs. In the case of the SNRs in the LMC, all stars within the searched area can be taken as being at the same distance,

coinciding with that of the SNR. In the Galactic case, since the stars in the sample to be studied are physically unrelated, before the advent of the *Gaia* space mission the distances had to be determined star by star, based on comparison of their spectra with photometric measurements.

Spectra are needed in all cases to measure radial and rotational velocities, looking for kinematic peculiarity. Large telescopes are required for that. The 10m *Keck* and *Subaru* telescopes in Hawaii and the 4.2m William Herschel telescope in La Palma have been used in the case of SN 1572 (the only “historical” SN Ia that can be studied from the Northern Hemisphere). The 8.2m ESO VLT telescopes have dealt with the other two Galactic SNe Ia explored, SN 1006 and SN 1604, using multi-slit spectrographs. Only the *HST* can, at present, reach the sites of the SNe Ia in the LMC and this is for comparing the color and magnitude of possible companions with the expected values.

For the Galactic SN Ia potential surviving companions, radial velocities are directly measured from the spectra. With high-resolution spectra, the stellar atmosphere parameters of the surveyed stars are obtained by comparison with synthetic spectra. The stellar parameters are required for distance determinations and are obtained by modeling of the stellar spectra. Rotational velocities can be measured from high-resolution spectra as well.

Another point concerning the detection of anomalously high space velocities is what sets the comparison standards. The Besançon model of the Galaxy (Robin et al. 2003) has been used to that end in several studies. Another way to single out stars with peculiar motions is to use Toomre diagrams (plots of the velocities on the meridian plane of the Galaxy against those on the Galactic plane) in which the companion candidates are plotted together with representative samples of the different Galactic populations (thin and thick disc, bulge, halo). Here, the second data release of the *Gaia* space mission (*Gaia* DR2)

provides a new resource: to compare the velocities of the possible companions with the observed distribution of a large sample of stars at similar distances and positions on the sky. The scrutiny of kinematics of the stars through the *Gaia* DR2 is limited to distances of 2–3 kpc away from us.

The *Gaia* DR2 makes also possible to measure trigonometric parallaxes and proper motions for candidates to supernova companion, in the SNRs of the Galaxy, that are brighter than $G \simeq 20\text{--}21$ mag (*Gaia* white-light magnitudes). In particular, several studies have been made in some of the SNe Ia that we will present. The proper motions of *Gaia* are given in an absolute frame (the ICRS), whereas those from *HST* are always relative to a local frame. Comparison is possible (see for instance in Tycho; Ruiz-Lapuente et al. 2019).

All the precedent is meant for searches in SNRs that come from a thermonuclear explosion. Therefore, the first step in any search is to identify the SNR as a SNR coming either from a thermonuclear explosion or from a core collapse supernova.

3.2. Typing a SN Ia SNR

As already said, there are about 300 SN remnants in our Galaxy (Green 2014) and an undertermined number in the LMC. The number of unambiguously classified remnants (thermonuclear, SN Ia SNRs and core collapse CC, SN II, Ib SNRs), however, is much smaller. One early way of classifying them as SNe Ia remnants or as core collapse remnants was through their morphology. Highly asymmetric X-ray morphology is typical of core collapse remnants (Lopez et al 2011). There is, however, a much better classification which emerges from the Fe–K shell X-ray emission (6–7 keV band), as explained in Yamaguchi et al. (2014).

The Fe–K α centroid is in the red part of the spectrum in SN Ia remnants and in the

blue part in CC SNe (see Yamaguchi et al. 2014; Martinez–Rodriguez et al. 2017). To discriminate explosion properties amongst SNe Ia models, line flux ratios (Si $K\alpha$ /Fe $K\alpha$, S $K\alpha$ /Fe $K\alpha$, Ar $K\alpha$ /Fe $K\alpha$) are useful. It is even possible to discriminate the metallicity of the SN Ia remnants from other ratios involving the Cr and Mg abundances (Badenes et al. 2008).

The three youngest and closest Galactic SNRs of SN Ia (1006, Tycho and Kepler) have been studied very intensively in the context of possible stellar companions. We also include in Table 3 all SNe Ia with good X-ray data that have been classified as SNe Ia in our Galaxy and in the LMC. We will discuss them briefly. We start giving an extensive account of the three first mentioned SN Ia remnants.

3.3. SN 1572 (Tycho Brahe’s supernova)

The central region of the remnant of the SN that appeared in 1572 (also known as Tycho Brahe’s supernova) was the first to be explored in search of a possible surviving stellar companion of the SN (Ruiz–Lapuente et al. 2004). The 2.5m *Isaac Newton Telescope* (photometry), the 4.2m *William Herschel Telescope* (spectroscopy), and the 2.5m *Nordic Optical Telescope* (spectroscopy), at the observatories in the Canary Islands, were mainly used, as well as the *HST* (astrometry). Supplementary observations were made with the two 10m *Keck* telescopes (spectroscopy), in Hawaii.

The region searched was a circle of 39 arcsec radius (about 15% of the radius of the SNR), with the same center as the X-ray emission measured by the *Chandra* satellite (RA = 00 h, 25 min, 19.9 s; dec = 64°, 08′, 18.2″). The limiting apparent visual magnitude of the survey was $V = 22$. The distance to the SNR being ~ 3 kpc (2.83 ± 0.79 kpc in Ruiz–Lapuente 2004), and the visual extinction $A_V = 1.7 - 2.0$ mag, all main-sequence stars of spectral

Table 3: Distances, size and ages of the Ia SNRs

Name	Distance	Size (Radius)	Age
	(kpc)	(arcmin)	(years)
Kepler	5 ± 0.7	1.9	414
3C 397	$6.3 - 9.8$	1.7	$1350 - 1750$
Tycho	2.83 ± 0.79	4.3	446
RCW 86	2.5	21	1833
SN 1006	2.18 ± 0.08	15	1012
G1.9+0.3	8.5	0.8	~ 150
G272.2-3.2	$1 - 3.2$	10	8000
G337.2-0.7	$2.0 - 9.3$	3	~ 5000
G299.2-2.9	5	5	5000
G344.7-0.1	$6 - 14$	5	$3000 - 6000$
G352.7-0.1	7.5	3.5	~ 2200
N103B	50	0.2	~ 860
0509-67.5	50	0.27	~ 400
0519-69.0	50	0.3	~ 600
0548-70.4	50	0.9	10,000
DEM L71	50	0.7	~ 4700

References: Ruiz-Lapiente (2017); Yamaguchi, H., et al. (2015); Ruiz-Lapiente (2004); Bocchino et al. (2000); Winkler et al. (2014); Borkowski et al. (2017); McEntaffer et al. (2013); Rakowski et al. (2003); Post et al. (2014); Giacani et al. (2011); Sezer & Gök (2014); Sano et al. (2018); Litke, Chu & Holmes (2017); Edwards, Pagnotta & Schaefer (2012); Hendrick, Borkowski & Reynolds (2003); Hughes, Hayashi & Koyama (1998); Kinugasa et al. (1998).

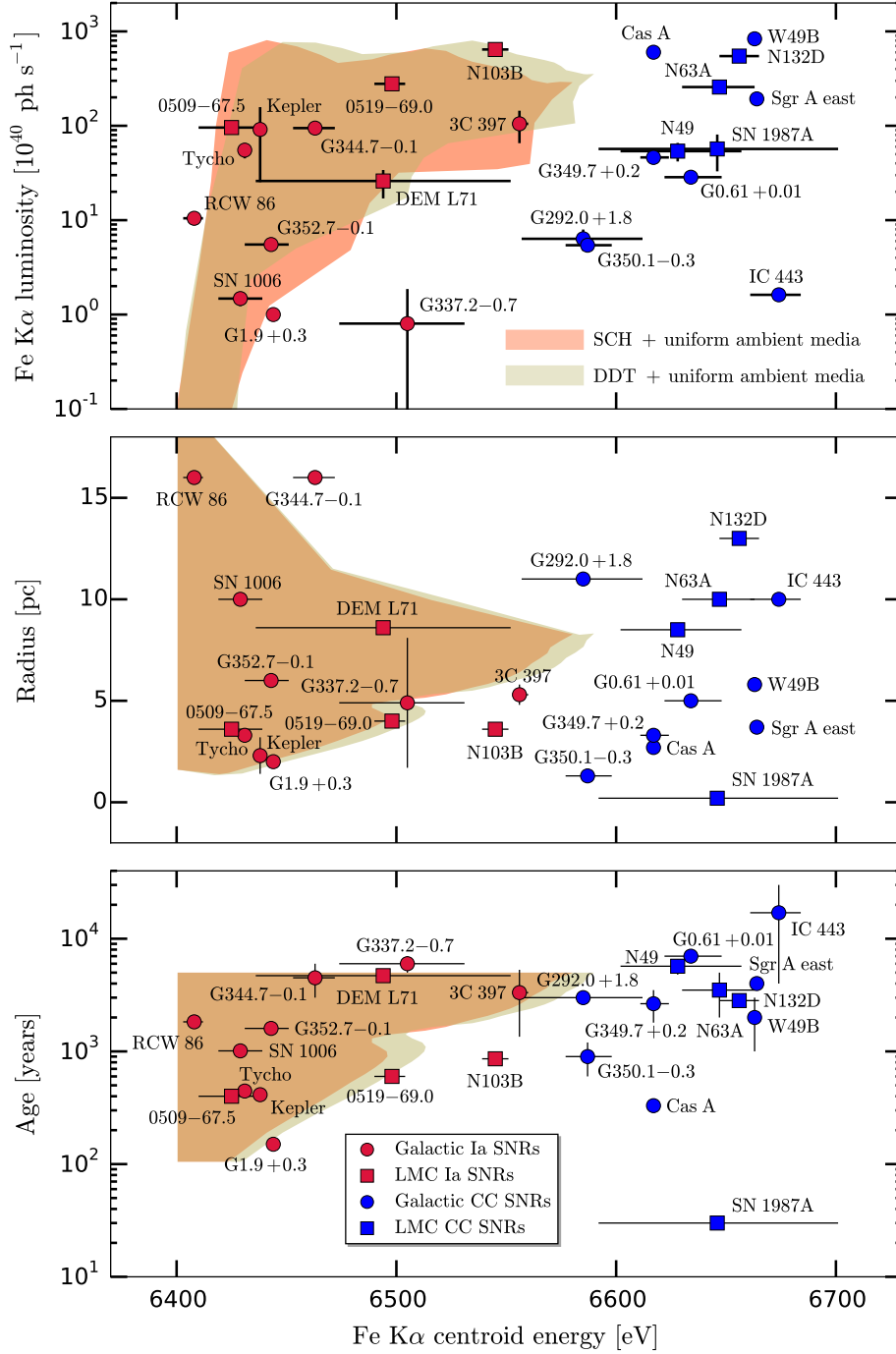


Fig. 6.— Fe K α luminosity, radius and expansion age as a function of the Fe K α centroid energy for Ia (red) and CC (blue) SNRs. The shaded regions depict the predictions from the theoretical MCh (khaki) and sub-MCh (dark orange) models with uniform ISM densities of Martínez–Rodríguez et al. (2018). (Courtesy of Hector Martínez–Rodríguez and Carles Badenes. ©AAS. Reproduced with permission).

type earlier than *K6* must have been detected (the Sun would appear, from there, as a $V = 18.9$ mag star).

The distances to the stars were determined from their spectral types and luminosity classes as compared with their visual magnitudes, taking into account extinction. Radial velocities were measured from the spectra and proper motions from the *HST* images (using the *WFPC2*). No chemical abundance analysis was attempted for any of the observed stars, just the metallicity being estimated. No rotational velocities were obtained, either.

Of the stars at distances compatible with Tycho’s SNR, one star, labeled *G* (located at 29.7 arcsec to the SE of the adopted center of the SNR) had an unusually high radial velocity (later refined to $v_r = -80 \pm 0.5$ km s⁻¹, by González Hernández et al. 2009, or to -79 ± 2 km s⁻¹, by Kerzendorf et al. 2009, both velocities in the LSR), to be compared with an average velocity $v_r = -20$ to -40 km s⁻¹, with a ~ 20 km s⁻¹ dispersion, at the distance and position of the SNR. The proper motions were found to be $\mu_b = -6.11 \pm 1.34$ mas yr⁻¹, perpendicularly to the Galactic plane, and $\mu_l = -2.6 \pm 1.34$ mas yr⁻¹, parallel to it. At the distance of the SNR, that would mean a tangential velocity of 94 ± 27 km s⁻¹. The modulus of the total velocity vector (radial plus tangential), would be 136 km s⁻¹, a factor of 3 larger than the mean velocity at 3 kpc, according to approximative estimates.

The atmosphere parameters of star *G* were $T_{eff} = 5,750$ K, $\log g$ between 3 and 4, and metallicity close to solar (its lower limit was $[M/H] > -0.5$). That corresponded to a G0–G2 subgiant of mass about $1 M_\odot$ and radius $R = 1 - 3 R_\odot$. The star, before the explosion, might either have been a main–sequence star, now still puffed–up after the SN impact, or a subgiant with a larger mass.

Based on its kinematic peculiarity, its distance and its profile, Ruiz–Lapuente et al. (2004) pointed to star *G* as a likely candidate to have been the companion of SN 1572.

Such identification has later been disputed. Kerzendorf et al. (2009) objected that high rotational velocities must be a characteristic of the companions of SNe Ia. That was based on the fact that the companion should be co-rotating with the system, at the time of the explosion (that is, the rotation period being equal to the orbital period). The orbital period being short in a contact binary, one of its components being a white dwarf and the other a main-sequence star filling its Roche lobe, the companion would be a fast rotator, but star G rotates slowly: $v_{rot} \sin i \lesssim 6.6 \text{ km s}^{-1}$ (González Hernández et al. 2009) or $v_{rot} \sin i \lesssim 6 \text{ km s}^{-1}$ (Kerzendorf et al. 2013). In the Section on rotation above, however, we have discussed the reduction of the pre-explosion rotational velocity by the interaction with the SN ejecta. Based on that, Pan, Ricker & Taam (2012b) and Liu et al. (2013) argue that the slow rotation of star G does not discard it as a possible companion of the SN. However, Liu et al. (2013) find that, given the age of Tycho’s SNR, the rotational velocity of their most slowly rotating model ($\sim 25 \text{ km/s}$) after impact is still higher than the measured rotational velocity of star G. The models by Pan, Ricker & Taam (2012b; their Table 3) with low rotation are of bloated stars. One can argue then that the models do not fully reproduce the characteristics of Tycho G.

González Hernández et al. (2009), from a high-resolution *Keck-1/HIRES* spectrum refined the stellar parameters of star G: $T_{\text{eff}} = 5900 \pm 100 \text{ K}$, $\log g = 3.85 \pm 0.30$, $[\text{Fe}/\text{H}] = -0.05 \pm 0.09$. Also, a Ni overabundance relative to Fe, $[\text{Ni}/\text{Fe}] = 0.16 \pm 0.04$ was measured, about 3σ above the average value in Galactic disk stars (Ecuvillon et al. 2004, 2006; Gilli et al. 2006), which they attributed to pollution by the SN ejecta.

Kerzendorf et al. (2013), however, from the same *Keck* spectrum, derived $[\text{Ni}/\text{Fe}] = 0.07 \pm 0.04$ only. They attributed the difference to differences in equivalent width (EW) measurements of Ni lines, maybe related to continuum normalization and/or local continuum placement. They compared the ratio to that from the set of F- and G-dwarf

abundances of Bensby et al. (2005) and found that the value was not unusually high. From that, Kerzendorf et al. (2013) concluded that star G was likely a background star, unrelated to the SNR.

Bedin et al. (2014) have later redetermined the Ni abundance (again from the same spectrum), using automated tools to fit the continuum and measure the EWs of the Ni lines. They have also removed weak lines. They find $[\text{Ni}/\text{Fe}] = 0.10 \pm 0.05$. Thus, the three measurements are compatible with each other, within the errors. The latter abundance ratio, when compared with the Galactic trend from Neves et al. (2009) (different from that in Bensby et al. 2006), still appears to be almost 1.7σ above the trend. From that, these authors conclude that the probability of the combination of the peculiar motion with even that moderate overabundance, in a star unrelated to the SN, would still be very low. Also, in Bedin et al. (2014), accurate proper motions were determined, from *HST* astrometry, for 1148 stars in the central region of Tycho’s SNR. Proper motions for 16 of these stars had also been measured by Kerzendorf et al. (2013), with good agreement for the stars common to the two sets.

Star *G* is not the only star in the central region of Tycho’s SNR to have been proposed as a possible companion of the SN. Ihara et al. (2007) claimed that the spectrum of star *E* showed blueshifted Fe absorption lines, that they interpreted as due to absorption by the approaching part of the expanding SNR. Star *E*, however, from the parallax measured by the space mission *Gaia* data release DR2, is found to be far behind the SNR (though the parallax determination has a large errorbar) .

Kerzendorf et al.(2013) had pointed to star *B*. It is a peculiar A–star, exhibiting fast rotation and an unusual abundance pattern of low overall metallicity, $[\text{Fe}/\text{H}] = -1.1$, yet high abundances of C and O. It is a few arcsecs from the geometrical center of the SNR, and at an estimated distance consistent with that of the remnant. Its surface temperature is

$T_{\text{eff}} = 10,722$ K, $\log g = 4.13$, and $v_{\text{rot}} = 170$ km s $^{-1}$. The high rotational velocity, however, is not unusual for an A–star. The abundance pattern can be explained if Tycho B is, as it seems, a λ Bootis star (see, for instance, Paunzen 2004, for a review of their properties). The deficit in Fe–peak elements in this type of stars has been attributed to dust–grain formation by the more refractory elements and their ejection by radiation pressure, in an accretion disk around the star. In this way, the atmosphere of the λ Bootis stars would be depleted of Fe–peak elements while having solar or near–solar abundances of C, N, O and S. The presence of such accretion disk would indicate that the now single star was a member of a binary system. However, star B as candidate companion of SN 1572 does not fit the characteristics of an impacted star that would be contaminated by iron–peak elements and would have a kinematical imprint that is not found in the measured proper motions and radial velocities of star B.

More recently, Kerzendorf et al. (2018a) have obtained UV spectra of star B with the STIS low–resolution grating of the *HST*, in search of broad Fe II absorption features due to the SNR, which would have shown that the star was inside or behind the remnant. From their absence and a new luminosity distance to star B, Kerzendorf et al. (2018a) conclude that it is a foreground star. However, the data of the *Gaia* DR2 place it at a distance compatible with that of the Tycho SN, but the star, as already said, does not present any kinematic peculiarity.

There had already been restrictions set on the high energy emission of the progenitor systems of the SN Ia, based on the state of the interstellar medium of their host galaxies (Woods & Gilfanov 2013, 2014). If, in the single–degenerate channel for production of the SNe Ia, mass accretion by the WD that will eventually explode is mediated by thermonuclear burning, at its surface, of the material transferred from the companion star, that would generate luminous line emission which should be seen when observing the host

galaxies if the rate of production of SNe Ia through the SD channel were high. From that, Johansson et al. (2014, 2016) have concluded that this accretion model could only contribute by a few percent to the total SN Ia rate in passively evolving galaxies, where there are no longer hot stars feeding such emission. Woods et al. (2018) have now set restrictions to the temperatures and luminosities of the progenitors of individual SNRs of the Ia type, based on such expected line emission luminosity. In the case of Tycho’s SN, the SD scenario is also disfavored on these grounds (Woods et al. 2017).

Another point, concerning not only the case of Tycho but all the SNRs that have been or will be surveyed in search of surviving companions of SN Ia, is the exact location of the site of the explosion. A centroid of the remnant can always be found and serve as initial guide for the exploration, but there can be sizeable shifts between the centroid and the actual site. Even for a perfectly symmetric explosion, if the SN ejecta encounter a density gradient in the circumstellar or the interstellar medium, in some direction, the expansion will be slowed down as it escalades the positive gradient, and accelerated as it runs down the negative one, so the apparent center of the resulting SNR will be shifted towards the side of the decreasing densities. That has been shown by the hydrodynamical simulations of Williams et al. (2013), where the remnant keeps a round shape in spite of this asymmetry.

On the other hand, there can be initial asymmetry in the SN ejecta themselves, as illustrated by Winkler et al. (2005) in the case of SN 1006. The structure inferred from absorption observations of background objects gives an explosion center displaced from the geometrical center of the SNR by an angular distance $\approx 19\%$ of the remnant’s radius. In the case of Tycho, Krause et al. (2008), from the spectrum of the light echo of the SN, also suggest that the explosion was aspherical.

Xue & Schaefer (2015), from a combination of historical reconstruction and semianalytical, approximative hydrodynamics, place the explosion site of SN 1572 at 37 arcsec ($\approx 15\%$

of the SNR radius) to the NW of the geometrical center of the SNR. But more recently, Williams et al. (2016), by combining new measurements of the proper motions of the forward shock of the expanding material with hydrodynamical simulations, determine a site located 22.6 arcsec ($\approx 9.5\%$ of the radius) to the NE of the geometrical center. This is more consistent with the existence of a density gradient in the E–W direction in the interstellar medium, with the density increasing towards the E. The hydrodynamical simulations of Williams et al. (2016) assume spherical symmetry in the ejecta which, as we have seen, could not be true, that leaving an uncertainty range that does not allow to exclude any of the stars in the surveyed area.

Very recently, Ruiz-Lapuente et al. (2019) have used the data release DR2 of the *Gaia* space mission to reevaluate distances and proper motions of the stars in the Tycho field. They have looked at the stars within 1 degree from the centroid of the SNR, and at a distance compatible with it. They examine the stars comprised in an area four times larger than in the work in 2004. They find general agreement with the distances estimated previously, with some exceptions, though. Star G is found to be somewhat closer than in earlier measurements. A Toomre diagram (see Figure 7) shows that its kinematics is similar to that of thick disk stars, its chemical composition being typical of the thin disk, however. Only $\approx 0.8\%$ of stars share these characteristics. The orbits described in the Galaxy by representative stars of the sample and by stars G and U are calculated and compared. These two last stars reach, by far, the highest distances from the Galactic plane, the total velocity of star U being significantly smaller. The very large number of stars with precise distances and proper motions in the *Gaia* DR2 now allow to compare the proper motions of candidate stars with those of a huge sample of stars around the same position and within the same range of distances (see Figure 8). Only stars G and U lie more than 2σ above average. These authors conclude that if star G were not the SN companion, the DD channel should be preferred for the origin of Tycho’s SN.

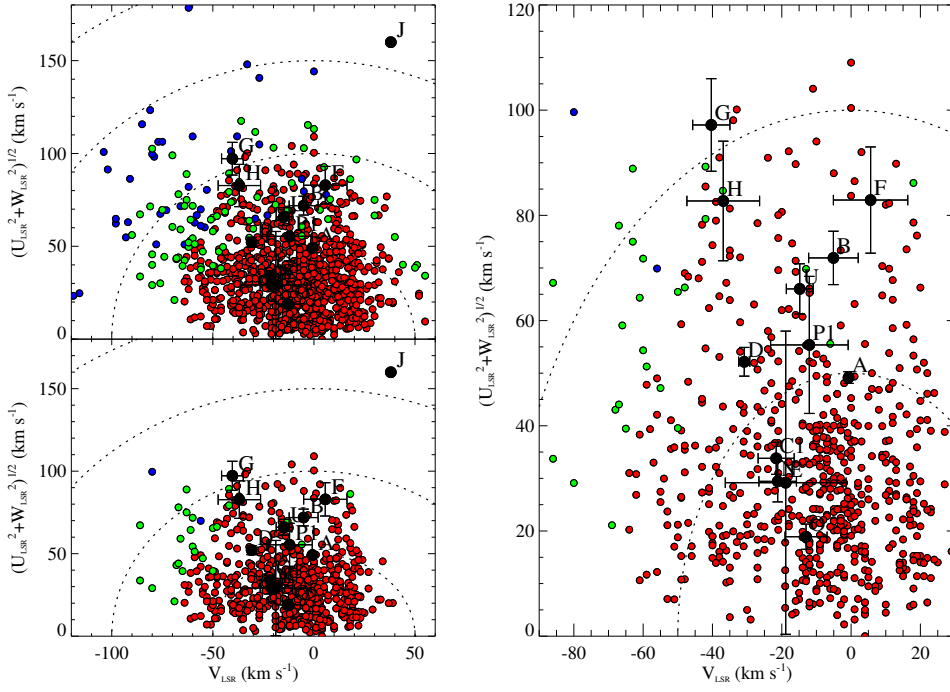


Fig. 7.— Left upper panel: Toomre diagram for a sample of thin disk, thick disk, and transition thin–thick disk stars, covering a wide range of metallicities, with stars in the Tycho field superimposed (red dots correspond to thin disk stars, green to transition, and blue to thick disk stars). Left lower panel: same as upper panel, keeping only stars with metallicities equal to or higher than that of star G. Right panel: detail of the lower left panel, leaving out star J, due to its large uncertainties in parallax and proper motions. The sample is taken from Adibekyan et al. (2012). (Ruiz-Lapuente et al. 2019. ©AAS. Reproduced with permission).

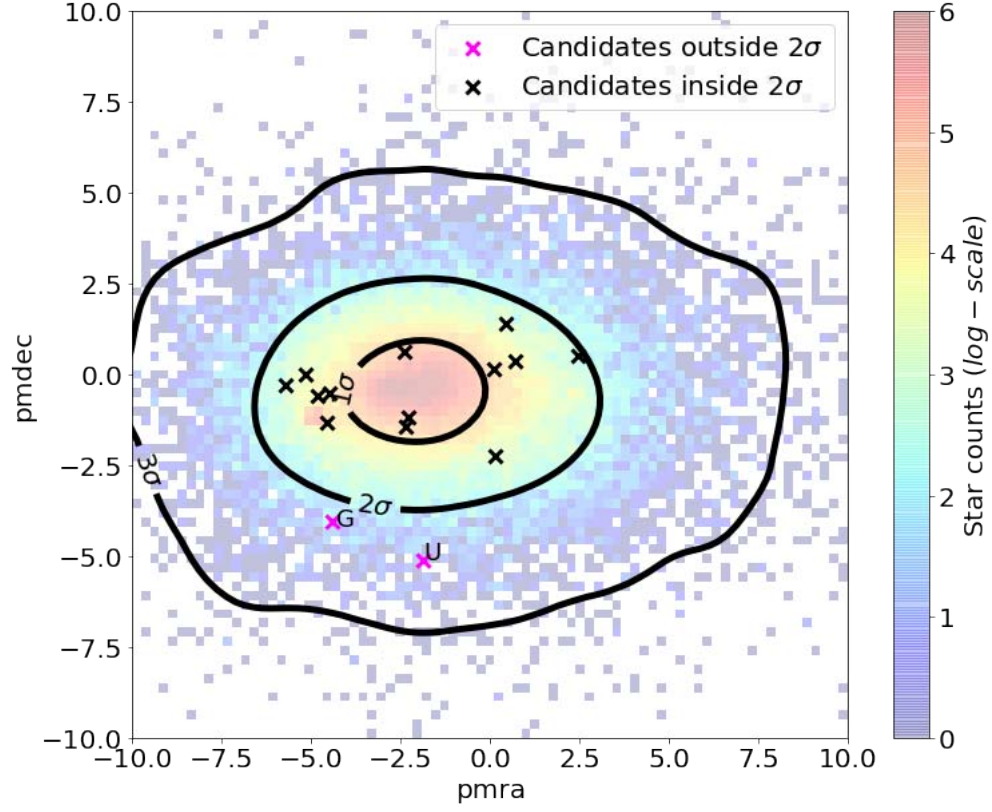


Fig. 8.— Proper motions of stars G and U, superimposed on those of a very large sample of stars around the same position and within the same range of distances. (Ruiz-Lapuente et al. 2019. ©AAS. Reproduced with permission).

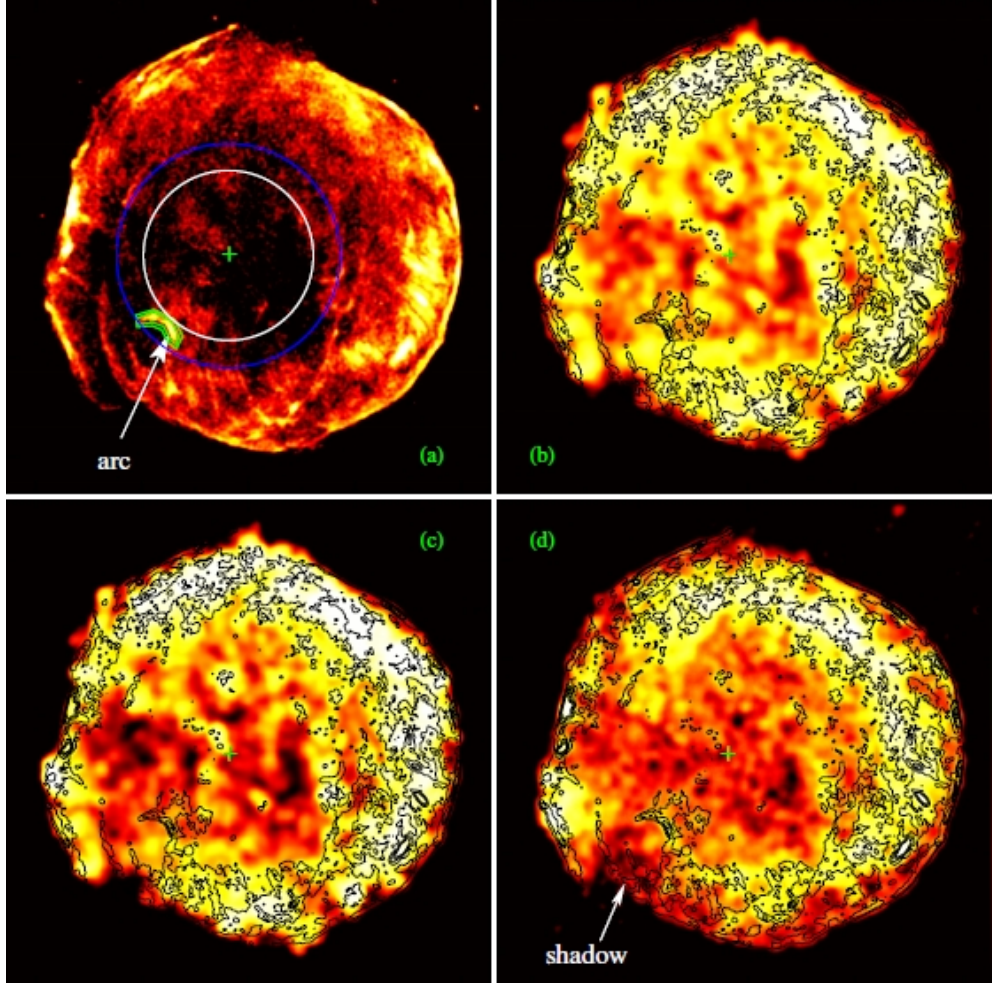


Fig. 9.— Chandra images of the Tycho SN remnant in four different energy bands. In the first panel, the arc attributed to the interaction of the SN ejecta with the companion is indicated. In the fourth panel the “shadow” in the emission that would be produced by the companion is also indicated. (Lu et. al. 2011). (Courtesy of Fangjun Lu @AAS. Reproduced with permission).

Lu et al. (2011) find a nonthermal X-ray feature in the SNR that seems to result from interaction between the SN ejecta and the stripped mass of the companion, aligned with the radial direction of Tycho G. They suggest this as a property favoring a SD origin of this SN. In this paper (Figure 9), and also as predicted in Marietta, Burrows & Fryxell (2000) and in García-Senz et al. (2012), the supernova ejecta intercepted by the companion leave a ”shadow” behind that is visible in X-rays. Zhou et al. (2016), from radio observations, find that Tycho is surrounded by a clumpy, expanding molecular bubble, whose origin would be a fast outflow driven from the vicinity of a WD as it accreted matter from a nondegenerate companion star.

The SD scenario for this supernova is still debated, however

3.4. SN 1006

SN 1006 has always been classified as a Type Ia supernova (see, for instance, Stephenson 2010). Its position on the sky ($\delta_{J2000} \simeq -42^\circ$) makes any deep study of its remnant only suitable for telescopes in the Southern Hemisphere.

The distance to the SNR has been determined, from the expansion velocity and the proper motion of the ejecta, to be $d = 2.18 \pm 0.08$ kpc (Winkler, Gupta & Long 2003). It is located about 500 pc above the Galactic plane. The interstellar extinction in the V-band is $A_V = 0.3$ mag only, much lower than in front of the two other historical Galactic remnants of SNe Ia, Tycho’s and Kepler SNRs.

The central region of the remnant of SN 1006 (see Figure 10) has been independently explored, in search for a possible surviving companion, by González Hernández et al. (2012) (GH12, from now on) and by Kerzendorf et al. (2012) (K12 henceforth).

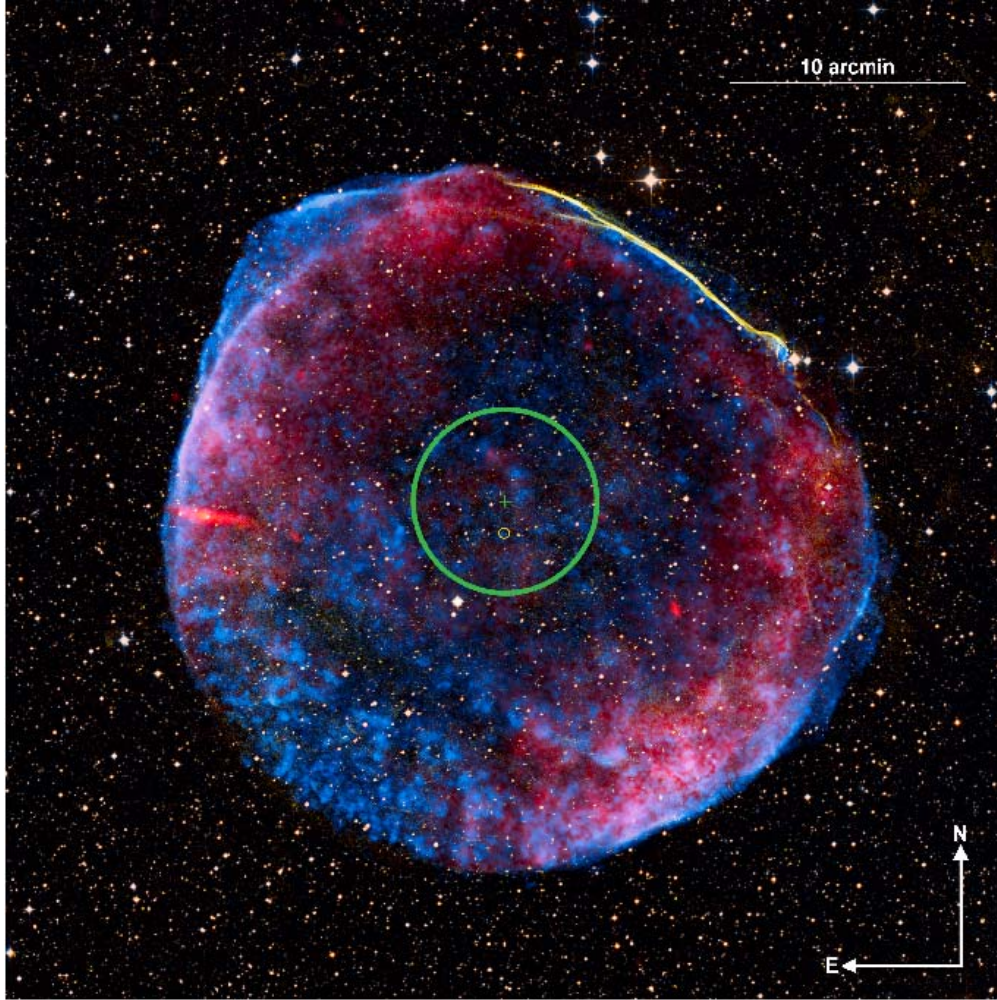


Fig. 10.— The remnant of SN 1006. The surveyed area in GH12 is indicated by the large green circle. The center of the survey (the centroid of the X-ray emission) is marked with a green cross, and that of the $H\alpha$ emission by the small yellow circle. The image is a composite of the X-ray, optical, and radio emissions (from GH12). (González Hernández et al. 2012. ©Springer Nature. Reproduced with permission).

The search by GH12 covered a circle of 4 arcmin radius around the geometrical center of the X-ray emission of the remnant determined by Allen, Petre & Gotthelf (2001): $\alpha_{J200} = 15^h 2^m 55^s$, $\delta_{J2000} = -41^\circ 55' 12''$. That radius amounts to 27% of the radius of the SNR (15 arcmin). K12 chose instead, for the center, a mean of the X-ray and radio centers, at $\alpha_{J2000} = 15^h 2^m 22^s.1$, $\delta_{J2000} = -41^\circ 55' 49''$, and a search radius of 2 arcmin. We must note, however, that Winkler et al. (2005), based on the distribution of the ejecta along the line of sight, propose a different center of the explosion, very close to the position of the Schweizer–Middleditch star, at $\alpha_{J2000} = 15^h 2^m 53^s.1$, $\delta_{J2000} = -41^\circ 59' 16''.7$. That is still inside the search radius of GH12, although close to the edge of the explored region.

The limiting magnitude of the GH12 survey, in the R-band, was $m_R = 15$ mag. Given the distance and the extinction, that included all red giants, subgiants and main-sequence stars down to $M_R = +3.1$ mag, but from the *Two Micron All-Sky Survey* (2MASS: Cutri et al. 2003) there are no main-sequence stars brighter than $m_R = 16.4$ mag in the explored field. That brings the limit down to $M_R = +4.5$ mag or, in the V-band, to $M_V = +4.9$ mag (stars only slightly less luminous than the Sun).

The K12 survey reached a limiting magnitude of $m_V = 17.5$ mag where they did full stellar modeling and a depth of $m_V = 19$ of stars for which they only probed the radial velocity. Given the distance and the extinction, $M_V = +5.5$ mag, and those limits are equivalent to half the Solar luminosity and a tenth of the solar luminosity, respectively. Thus, the GH12 survey was more extended than K12 (four times in the area covered) but the latter was deeper.

Both GH12 and K12 surveys were spectroscopic, although K12 had, in addition, done a previous run of photometric observations. In the two cases the *Very Large Telescope* of the *European Southern Observatory* was used, but with two different instruments: the high-resolution *Ultraviolet and Visual Echelle Spectrograph* (UVES) in GH12, and the *Fibre*

Large Array Multi Element Spectrograph (FLAMES) with the medium–high resolution *GIRAFFE* spectrograph in K12.

In the two surveys, the stellar parameters T_{eff} , $\log g$, and the metallicity $[\text{Fe}/\text{H}]$ were derived from the observed spectra, using similar techniques. In addition, GH12 also determined the chemical abundances of the Fe–peak elements Cr, Mn, Co and Ni, as well as those of Na and of the α –elements Mg, Si, Ca and Ti. The spectra equally provided the radial and rotational velocities of the stars.

Thanks to the high quality of the UVES spectra, the errors in the stellar parameters of GH12 are very small: from 30 to 100 K in T_{eff} , from 0.1 to 0.2 in $\log g$, and from 0.03 to 0.06 dex in $[\text{Fe}/\text{H}]$. The FLAMES/GIRAFFE spectra, instead, make the errors in K12 to be larger: 250 K in T_{eff} , 0.5 in $\log g$, and 0.5 dex in $[\text{Fe}/\text{H}]$.

No significant rotational velocities were found for any of the stars, neither in the GH12 nor in the K12 surveys.

As for the radial velocities, GH12 compared the observed velocities with the distribution predicted by the Besançon model of the Galaxy (Robin et al. 2003): all the stars in the sample were consistent with the model distribution, with no significant outlayer being found. GH12 compared the observed distribution of the abundances of Fe–peak elements as a function of metallicity with the Galactic trends (see Figure 11), in search for signs of chemical contamination of the surface of some star by the SN ejecta. All stars are within the dispersion of the Galactic trends. The same is true for the α –elements.

GH12 also use the stellar parameters derived for the sample stars, and the photometric magnitudes in five different filters from the *2MASS* catalogue, to determine the distances. Only four stars are at distances (marginally) compatible with that of the SNR. All of them are red giants, without any kinematic nor spectroscopic peculiarity.

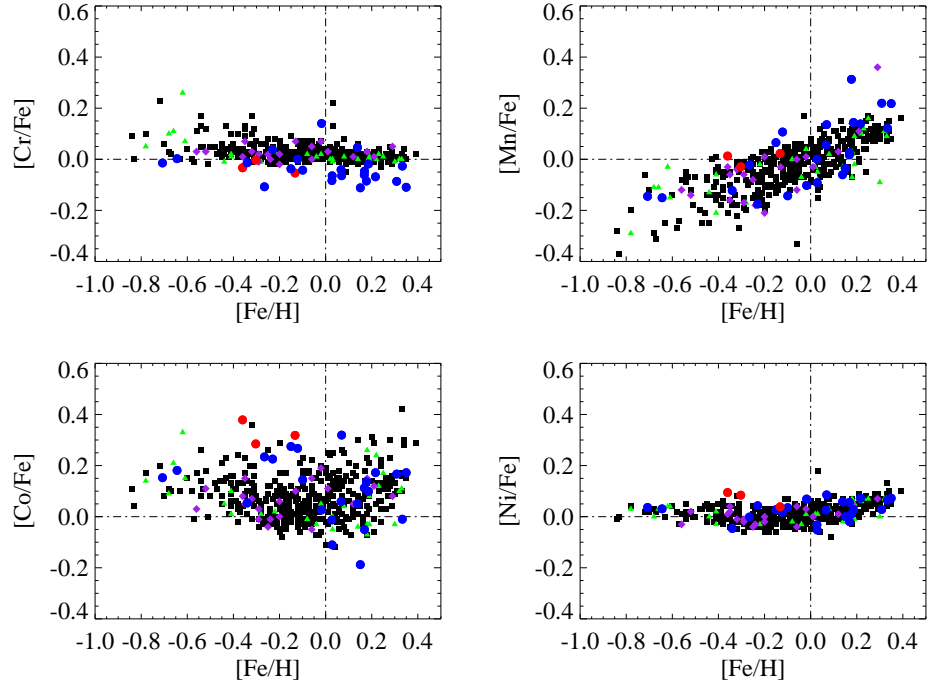


Fig. 11.— Stellar abundance ratios $[X/Fe]$ of several Fe-peak elements. Red triangles correspond to the four giant stars at distances compatible with that of the remnant of SN 1006. Blue squares, to the rest of the stars in the sample of GH12. (González Hernández et al. 2012. @Springer Nature. Reproduced with permission).

The conclusions of GH12 and K12 were the same: either the companion must have been an unevolved star, less luminous than the Sun, and having returned to its initial state only $\sim 1,000$ yr after the SN explosion (which appears very unlikely) or the explosion was due to the merging of two white dwarfs. In both papers, the possibility that the SN were produced through the spin-up/spin-down channel and then the companion would be a faint WD at the time of the explosion, was considered, arguments against it being given in GH12 and in subsection 2.4 of the present paper.

The spin-up/spin-down channel is not the only way to have a WD as a surviving companion of a SN Ia. As discussed above, Shen & Schwab (2017) have considered the case of He detonations close to the surface of a mass-accreting C+O WD, induced by mass transfer from a He WD or a less massive C+O WD. The He detonation might then compress enough the core of the WD to induce a second detonation there, and the mass donor would be flung at its orbital velocity and survive. ^{56}Ni -rich material might be captured by those WDs and its decay induce the emission of stellar winds from their surfaces. The WDs, at times after the explosion comparable with the age of SN 1006, would be hot UV sources, with luminosities $\sim 1 L_{\odot}$.

Kerzendorf et al. (2018b) have made a deep photometric search of the remnant of SN 1006, using the Dark Energy Camera (DECam) of the Dark Energy Survey on the 4m Blanco telescope located at Cerro Tololo Inter-American Observatory. They compare the observations with both the predictions from the models of Shen & Schwab (2017) and with WD cooling sequences. The latter comparison excludes WDs with cooling ages $\lesssim 10^8$ yr. The observations equally rule out the hot WD models resulting from radioactive decays taking place at their surfaces (Figure 12). Kerzendorf et al. (2018) can also rule out most spin-up/spin-down models as the only possible WD that could escape detection must be older than $\approx 10^8$ yr.

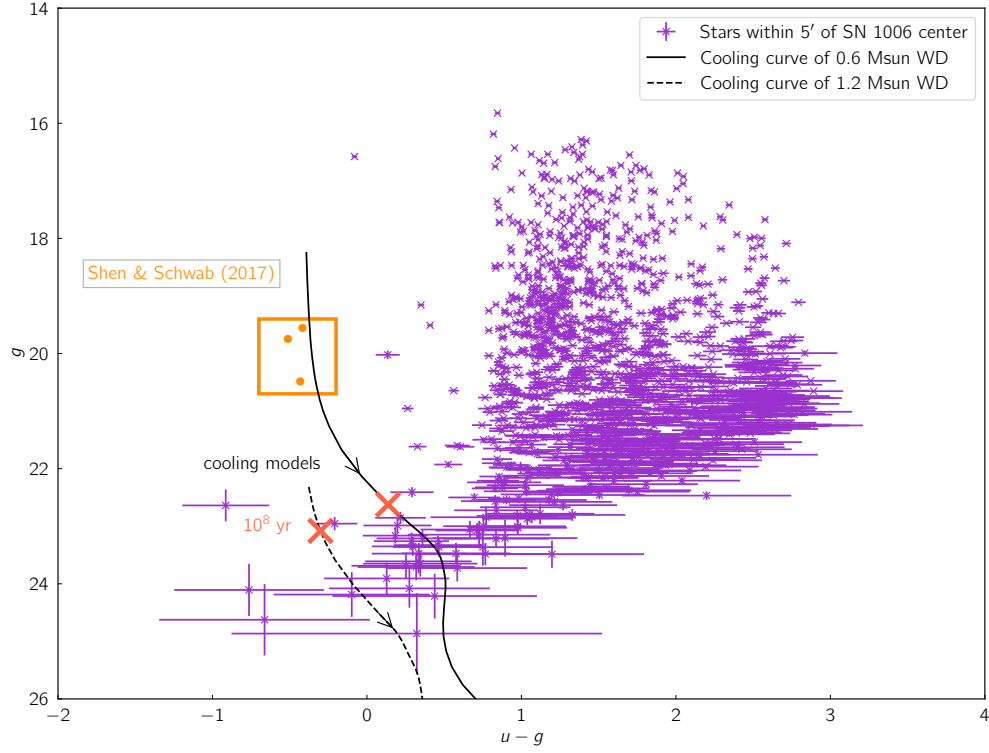


Fig. 12.— This Figure is taken from Kerzendorf et al. 2017 (Figure 2). WD cooling curves (solid: $0.6 M_{\odot}$, dashed: $1.2 M_{\odot}$; Tremblay et al. 2011). The data are a color-magnitude diagram (CMD) of all DECam stars within 5 arcmin from the center. In orange, the models by Shen & Schwab (2017). (@MNRAS Permission granted).

3.5. SN 1604 (Kepler’s supernova)

The classification of SN 1604 as SN Ia has been long debated, some authors ascribing it to the core-collapse mechanism (Bandiera 1987). X-ray observations of the remnant (Cassam-Chenaï et al. 2004) showed that the O/Fe ratio was characteristic of SNe Ia (see also Reynoso et al. 2007). More recently, Ruiz-Lapuente (2017) has reconstructed, from the historical records left by European, Korean and Chinese astronomers, the light curve of the SN, finding that it was a normal SN Ia.

The distance to the remnant of SN 1604 has also been the subject of discussion, but there is now general agreement that it is ~ 5 kpc (Sankrit et al. 2016; Ruiz-Lapuente 2017). The remnant appears to be expanding from a center located at $\alpha_{J2000} = 17^h30^m41^s.321 \pm 41^s.4$ and $\delta_{J2000} = -21^\circ39'30''.51 \pm 4''.3$ (Sato & Hughes 2017). The Galactic latitude being $b = 6^\circ.8$, it lies $\simeq 590$ pc above the Galactic plane. The field is heavily obscured, the extinction being $A_V = 2.7 \pm 0.1$ mag (Blair et al. 1991; Schlafly & Finkbeiner 2011).

Concerning the circumstellar medium of SN 1604, Vink (2008) finds that one of the components of the binary system that gave rise to the SN might have created a shell of $\sim 1 M_\odot$, expanding into the interstellar medium. According to Katsuda et al. (2015) the shell would have lost contact with the binary years before the explosion. Chiotellis et al. (2012) and Vink (2017) suggest that the companion was an AGB star that had lost its envelope at the time of the explosion.

Kerzendorf et al. (2014) made the first exploration of the central region of Kepler’s SNR. The search was photometric and spectroscopic, covering a square field of $38'' \times 38''$ around the center of the remnant determined by Katsuda et al. (2008) (only slightly differing, in declination, from the above estimate by Sato & Hughes, 2017). The limiting apparent magnitude of the survey was $m_V \simeq 18$ mag. Given the distance and the extinction, that

means reaching a limiting luminosity $L \simeq 6 L_{\odot}$. The WiFeS-spectrograph on the 2.3m telescope of the Australian National University was used for the spectroscopy and archival *HST* images for the photometry.

24 stars were found within the explored area and the magnitude limit of the survey. From the *HST* images, their magnitudes in the F550M filter range from 17.24 to 19.24 mag. For 13 of them, there are also V magnitudes taken from the *Naval Observatory Merged Astrometric Data (NOMAD)* catalogue, that range between 15.9 and 17.7 mag. From Table 1 in Kerzendorf et al. (2014), the star with the lowest luminosity (in the V filter) in the sample had $L = 7 L_{\odot}$.

The quality of the spectra did not allow to infer the stellar atmosphere parameters and, as a consequence, no comparison of the absolute magnitudes corresponding to them with the photometry was possible, so the distances remained unknown.

Only radial velocities could be measured, for most of the stars (18 of them, according with their Table 2), with a typical error of $\approx 4.5 \text{ km s}^{-1}$. No rotational velocity could be determined to better than 200 km s^{-1} , instead. Kerzendorf et al. (2014) then compared the radial velocities found with those given by the Besançon model of the Galaxy (Robin et al. 2003) for the distribution of such velocities at the distance and position of the SNR, and also with the predictions of Han (2008) for the velocities of the ejected companions of SNe Ia. They found no star significantly deviating from the Besançon model. On the other hand, half of the stars in the velocity distribution deduced from Han (2008) would appear as significant outliers in that model. They did not find any clear candidate to be the surviving star of the explosion.

From comparison of the observed brightnesses with predicted luminosities, Kerzendorf et al. (2014) could discard red giants as possible surviving SN companions in Kepler’s SNR.

That was already an important point, given the previous suggestions (see above), from the characteristics of the circumstellar medium, that the companion was an AGB star.

More recently, Ruiz-Lapuente et al. (2018) have made a new exploration of the central region of Kepler’s SNR. They have surveyed a circle of 24 arcsec radius around the center of the remnant given by Vink (2008), which is practically coincident with that from Sato & Hughes (2017), down to an apparent magnitude $m_R = 19$ mag which, given the distance and the extinction, translates into an absolute magnitude $M_R = 3.4$ mag or a luminosity $L = 2.6 L_\odot$. The survey includes spectroscopy with the multiobject spectrograph *FLAMES* on the 8.2m ESO VLT–UT2 and proper motions from images taken by the *HST*, with a baseline of 10 yr. The initial search radius was expanded to 38 arcsec to take advantage of free fibers in *FLAMES* although the extra stars are too distant from the center of the SNR. A total of 32 stars were observed.

Proper motions for all 32 stars were measured (Figure 2 and Table 3 in Ruiz–Lapuente et al. 2018b). The number of surveyed stars is much larger, however, and the astrometric sample can be considered complete down to $m_{F814W} \simeq 22.5$ mag (wide *I*) and 50% complete down to $m_{F814W} \sim 23.4$ (see the rightmost panel in Figure 3 of that paper).

The stellar parameters T_{eff} , $\log g$, and $[\text{Fe}/\text{H}]$ were determined from the spectra obtained. The *FLAMES* observations had been made in the Combined IFU/7–Fiber simultaneous calibration UVES mode and Giraffe using the HR9 and HR15n settings. Two stars were observed both in UVES and Giraffe, thus providing a reliability test of the observations. The stellar parameters were derived from a set of narrow–band spectral indices, following the method described in Damiani et al. (2014). Then, the distances to the stars were determined from comparison of the deduced absolute magnitudes M_V , M_R , M_J , M_H , and M_K with the photometry of the *NOMAD* catalog, taking into account the corresponding extinctions (Table 5 in Ruiz–Lapuente et al. 2018b). The results suggest that the sample

is made of an ordinary mixture of field stars (mostly giants). A few stars seem to have low metallicities ($[\text{Fe}/\text{H}] < -1$) but with large error bars, and they are all consistent with being metal-poor giants.

Radial and projected rotational velocities ($v \sin i$) were measured from the spectra, with errors of $1\text{--}2 \text{ km s}^{-1}$ in v_r and of $10\text{--}15 \text{ km s}^{-1}$ in $v \sin i$. The radial velocities are compared with those obtained by Kerzendorf et al. (2014), for the stars in common between the two samples. There is reasonable agreement in most cases and some unexplained significant discrepancies in a few of them.

The measured radial velocities and proper motions are plotted over the corresponding distributions given by the Besançon model of the Galaxy, for the 12 stars at distances shorter than 10 kpc, in Figures 5–7 of Ruiz-Lapuente et al. (2018). There are no significant outliers. One star (T18 in that paper, which is A1 in Kerzendorf et al. 2014) has a very large proper motion, but it is an M star at a distance of 0.4 kpc only. This distance is obtained from stellar modeling and confirmed by the *Gaia* DR2 parallaxes.

Ruiz-Lapuente et al. (2018) conclude that from the absence of any peculiar star down to $\approx 2 L_{\odot}$ and within an angular distance from the center of the SNR amounting to 20% of the average radius of the remnant, the single-degenerate channel appears clearly disfavoured in the case of Kepler’s SN. There is agreement in that with Kerzendorf et al. (2014). Given the characteristics of the circumstellar medium, with a massive shell expanding from the site of the explosion, the core-degenerate channel (Kashi & Soker 2011) appears favored: a WD merging with the also electron-degenerate core of a red giant star inside an AGB envelope.

3.6. RCW86

RCW86 (also known as G315.4-2.3 or MSH14-63) is the result of a SN explosion that is thought to correspond to the “guest star” of 185 A.D. observed by Chinese astronomers (Clark and Stephenson 1977). This SNR has a radially oriented magnetic field similar to those of Tycho, Cas A, and Kepler, which confirms its relative youth (Petruk 1999). Its distance is very well known, with values comprised between 2.3 kpc (Sollerman et al. 2003) and 2.8 kpc (Rosado et al. 1996).

From both radio and X-ray observations, its shape is close to spherical, with an angular diameter varying between 40 and 43 arcmin.

An inconvenience is its large diameter: 29 ± 6 pc, which implies, at a distance of 2.5 kpc, a $4'$ radius to enclose 20 % of the inner core. More adequate than a 20 % of the inner core is a 40 %, given the ill-definition of the remnant (Williams et al. 2011; Lopez et al. 2011; see Figure 13).

3.7. Other Galactic SNe Ia under scrutiny

We now address the steps to clarify the origin of other Galactic SN Ia remnants. The ejecta of some of these SNe are appreciably asymmetric, the diameter of the remnant being different in the E–W direction than in the the N–S direction. The origin of the asymmetry is unclear: it might either be caused by the explosion mechanism such as off-center ignitions or to double detonation in the exploding white dwarf (Maeda et al. 2010; Fink et al. 2010), to expansion through a nonuniform medium along the line of sight, or to expansion altered by a circumstellar medium modified by planetary nebula-like bipolar outflows from the companion star of the SN (Tsebrenko & Soker 2013).



Fig. 13.— Combined image of RCW86, from X-rays (*XMM Newton* and *Chandra*) and infrared data (*Spitzer Space Telescope Observatory* and *Wide-Field Infrared Survey Explorer*). X-rays are in blue and green. Infrared emission, in yellow and red. Public Domain.

3C 397 is one of the brightest Galactic SNR in radio and it has an irregular shape. Yamaguchi et al. (2015) presented *Suzaku* X-ray spectroscopic observations detecting high abundances of Ni and Mn. They infer in their analysis that this was the explosion of a SN Ia close to the Chandrasekhar mass. This is found as well in the study by Dave et al. (2017), that suggests that this SN Ia falls well into the single degenerate scenario, where a central deflagration is induced by accretion of mass from a non-degenerate companion. The deflagration would turn into detonation in the WD, according to this analysis. It is possible to test if there was a companion or not, though this requires at the moment a photometric and kinematic characterization. The distance of *3C 397* is in the range of 6.3–9.7 kpc and its age is estimated to be around 1350 yr–1750 yr (Leahy & Ranasinghe 2016). It occupies in the sky around ~ 1.7 arcmin in radius. It is not an easy search due to the fact that this remnant is on the plane of the Galaxy and the extinction is very large. So, it should be postponed to a possible examination with the NIRcam on board of the *JWST* and give it a lower priority in front of other remnants.

G344.7-0.1 SN remnant was discovered in radio observations (Caswell et al. 1975) and has a largely asymmetric structure with a diameter of ~ 10 arcmin. X-ray observations made from the *Suzaku* satellite (Yamaguchi et al. 2012) have shown strong K-shell emission from lowly ionized Fe, and the pattern of abundances is consistent with a SN Ia origin. The distance to this SNR is uncertain, a value between 6 and 14 kpc (Giacani et al. 2011, Yamaguchi et al. 2012). It seems clear that it is located in the opposite edge of the Galactic plane, beyond the Galactic center (Yamaguchi et al. 2012). Its age is estimated to be between 3000 and 6000 yr. A more detailed X-ray analysis is needed. More detailed constraints on its age are required to limit the companion search in this SN Ia SNR. However, this search is perhaps not proritary when compared with other studies. The distance is larger (6–14 kpc) than to other remnants and that entails a greater difficulty for gathering the information required for the identification of the surviving companion. In addition, it is

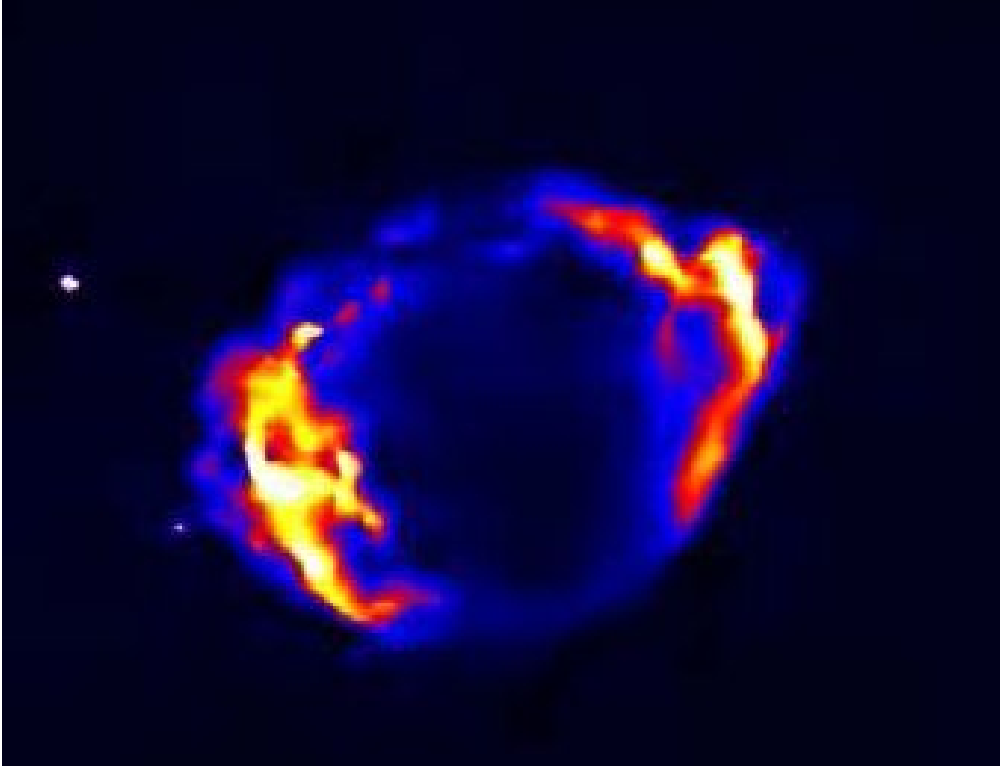


Fig. 14.— Image in X-rays of G1.9+0.3. It is worth reminding that this image is of a remnant of only 50 arcsec of radius. The search radius could encompass stars within the 10 arcsec radius (20% of that of the SNR). Image adapted from Borkowski et al. (2017). (Courtesy of Kazik Borkowski. ©AAS. Reproduced with permission).

highly extinguished, being very close to the Galactic plane.

G352.7-0.1 SN remnant is asymmetric, with radius around 3.9 arcmin (Sezer & Gök 2014) and elemental abundances that are typical of a SN Ia remnant. Its age is ~ 2200 yr and the distance is estimated to be around 7.5 ± 0.5 kpc by studying the interstellar gas surrounding it (Giacani et al. 2009). Its location is very close to the Galactic plane. The age of the remnant and the shorter distance makes it a better case than the previous remnant for a survey in the infrared with the *JWST*.

G337.2-0.7. Here again we have an SN Ia remnant asymmetric with size of 4.5×5.5 arcmin (diameter). The models by Badenes et al. (2003) fitting the X-ray spectrum of this remnant give an estimate of its age of 5000 years and an uncertain distance between 2–9.3 kpc (Rakowski et al. 2006). This remnant, though close to the Galactic plane, is a bit higher and has a smaller extinction than the three remnants previously addressed. Though, from the series of remnants that we are discussing, the really priority one for a search for a companion with the *JWST* is the next remnant that we are about to introduce.

G1.9+0.3 was discovered in 2008, and it is believed to be the remnant of a SN Ia which exploded around 1900. The supernova is 8.5 kpc away from us (Carlton et al. 2011) and has only 50 arcsec of radius. However, it is highly extinguished in the optical. Studies of how much would the absorption in the infrared be (Reynolds et al. 2008) set an infrared absorption of the order of 1.8 mag in the K band. This is consistent with what is obtained from the Besançon model of the Galaxy (Robin et al. 2003). The fact that this SNR is so recent means that the companion star, even moving at 400 km s^{-1} perpendicularly to the line of sight, would only be 1.2 arcsec away from the site of explosion after the 120 years elapsed since the event. Thus a search could include the study of stars within 10 arcsec of radius, to allow for the possible difference between the expanding center of the SNR and the explosion site. It could even be enlarged to 30% and that would be 15 arcsec of radius

around the expansion center. Never before such a small circle of search had been enough for a conservative exploration of companion candidates in a SNR in our Galaxy. Thus, this SNR offers an exceptional opportunity. One will not have hundreds of candidates to examine, as in other cases, but only a reasonable amount (see Figure 14).

Chakraborti et al. (2016) have studied this very young SNR. They find that circumstellar interaction in young Galactic SNRs can be used to distinguish between SD and DD progenitor scenarios. The X-ray flux and the size of the remnant are both increasing, and these authors introduce a *surface brightness index*, relating flux and size evolution. The theoretical evolution of this index is different in the two scenarios, and it is always negative in the SD case (no simultaneous increase in flux and size). Since the contrary is observed in the SNR G1.9+03 case, they favour the DD scenario there: no candidates should be found.

Now, we come to 2 SN Ia remnants that are not highly extinguished and nearby. They present a very good opportunity to look for the surviving companion of those SNe Ia.

G299.2-2.9. This SNR was discovered, in X-rays, by Busser, Egger & Aschenbach (1995), as a part of the *ROSAT All Sky Survey*. *Chandra* observations have provided measurements of abundance ratios in good agreement with the predictions of delayed-detonation models of SNe Ia (Post et al. 2014; Park & Post 2016). The distance seems to be ~ 5 kpc, and the age $\sim 4,500$ yr (Park et al. 2007; Park & Post 2016). The coordinates of the centroid of the X-ray emission are $RA = 12^h 14^m 50^s.508$; $Dec = -65^\circ 28' 14''.51$ (J2000) (Post 2017; see Figure 15). This corresponds to Galactic coordinates $l = 299.142^\circ$ and $b = -2.869^\circ$. Thus, this SNR is below the Galactic plane. Its estimated extinction, $A_V = 2.3$, is moderate (if we take into account the whole sample of Galactic SN Ia SNRs) and enables to construct color-magnitude diagrams in search of a possible surviving companion. Other SN Ia SNRs have been studied with color-magnitude diagrams, as seen in the section on SN 1006 and will be shown in the section on LMC SNRs. Those comparisons have been



Fig. 15.— Three-color image of G299.2–2.9, based on *Chandra* data. Red, green and blue represent the 0.4–0.72; 0.72–1.4, and 1.4–3.0 keV bands, respectively. (Courtesy of Sangwook Park. @AAS. Reproduced with permission).

centered on companions of the MS and the He star types studied by Pan et al. (2014). In addition to the classical MS, subgiant and red giant companions impacted by the explosion, we would like to extend the searches to types of possible surviving companions that have not yet been investigated.

sdB companions would typically have $L \simeq 10 L_{\odot}$ and $T_{\text{eff}} \simeq 40000K$. With an interstellar extinction $A_U = 3.6$ mag (Schlafly & Finkelbeiner 2001) and for a distance ~ 5 kpc, we have $m_U \simeq 22.5$ mag, so going to a U magnitude of 23 should cover these possible hot companions, not searched for in any other SNR yet. To cover the faint companions up to $L \simeq 0.01 L_{\odot}$, with an extinction $A_V = 2.3$ mag, we should go, at the distance of the SNR, to $m_V = 25.7$ mag. Therefore, reaching down to 26 mag in the V and R bands would be required.

G272.2-3.2. It was discovered in the ROSAT All-Sky Survey (Greiner & Egger 1993), and more recently studied by Harrus et al. (2001) and McEntaffer et al. (2013). It was produced by a SN Ia explosion (Lopez et al. 2011) and it is 6000–12000 yr old. The centroid position is $\alpha_{J200} = 09^h 06^m 45^s.7$, $\delta_{J2000} = -52^{\circ} 07' 03''$ (Greiner & Egger 1993) and $l = 272.13^{\circ}$, $b = -3.19^{\circ}$. It is far enough from the plane of the Galaxy so that, as in the previous case, it can be studied through color–magnitude diagrams. The distance is $d = 1.8_{-0.8}^{+1.4}$ kpc (Greiner et al. 1994), or ~ 2 –2.5 kpc according to Harrus et al. (2001) and Kamitsukasa et al. (2016). Its distance from the Galactic plane, at 2 kpc, would be over 110 pc. The diameter of the remnant is slightly less than 20 arcmin. This SNR has a extinction somehow larger than the previous one. Then, the estimated requirement to cover the colour–magnitude diagrams and to study all the abovementioned possible companions, means to go as deep in magnitude as in the previous remnant G299.2-2.9.

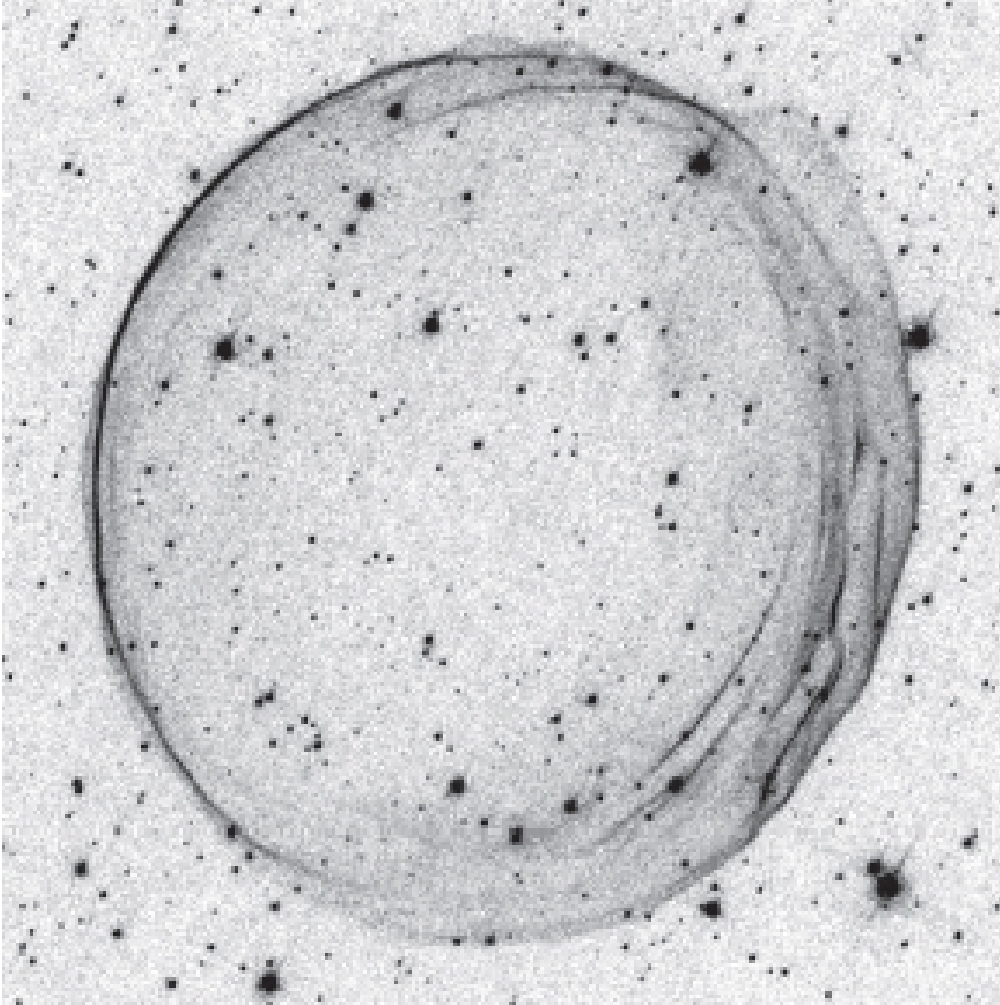


Fig. 16.— SNR 0509-67.5 in the $H\alpha$ filter, obtained by the ACS on board *HST* (from Hovey, Hughes & Ericksen 2015). (Courtesy of Luke Hovey & Jack Hughes. ©AAS. Reproduced with permission).

3.8. Type Ia supernovae in the Large Magellanic Cloud

Twelve SNRs in the Large Magellanic Cloud (LMC) have been identified as being produced by SNe Ia (Litke et al. 2017, and references therein). Only five of them have been explored to date.

The first remnant to be studied in search for a surviving companion was SNR 0509-67.5 (Schaefer & Pagnotta 2012). This SNR was discovered as an X-ray source by the *Einstein Observatory* (Long et al. 1981) and confirmed as a SNR by Tuhoy et al. (1982). Later, an SN Ia origin was indicated by *Chandra* X-ray observations (Warren & Hughes 2004) showing that the ejecta abundances were consistent with the nucleosynthesis predictions for delayed-detonation models of SNe Ia. Rest et al. (2005) discovered light echoes, based on which the SNR has an age of 400 ± 120 yr. Optical spectra of the light echoes (Rest et al. 2008) showed that the explosion was a SN Ia, likely overluminous as SN 1991T.

From images taken with the *HST*, no possible companion star was found down to an apparent magnitude $V = 26.9$ mag (corresponding to an absolute magnitude $M_V = +8.4$ mag and thus to about $0.04 L_\odot$). The authors explored an error circle with $1.43''$ radius around the apparent center of the remnant, which they deemed sufficient from the estimate of the maximum angular distance that the fastest possible companions (main-sequence stars) might have travelled in ≈ 500 yr (the upper 3σ error in the calculated age of the SNR). From that, they concluded that the SN should have been produced through the DD channel.

Such conclusion was challenged by Di Stefano & Kilic (2012), based on the spin-up/spin-down mechanism (see above). They argued that the spin-down time might have been long enough for the companion to have become a WD, dimmer than the limiting magnitude reached in the exploration of Schaefer & Pagnotta (2012). The time scale of spin-down was

later addressed by Meng & Podsiadlowski (2013) (see also above), who found that it might have been sufficient for a red-giant companion to become faint enough to have escaped detection.

Di Stefano & Kilic (2012) also argued that the region explored might have been too small, given the possible degree of discrepancy between the geometric center of the SNR and the actual site of the explosion.

Hovey, Hughes & Eriksen (2015) (see Figure 16), using narrow-band $H\alpha$ images taken with the *HST*, made proper motion measurements of the forward shock of the remnant. They found asymmetry in the expansion velocity along an approximate E–W axis. Hovey (2016), and Hovey, Hughes & Eriksen (2016), combining these proper motion measurements with hydrodynamical modeling, calculated the offset of the explosion site from the geometric center of the SNR, based on different assumptions. From that, they derived a search radius significantly larger than the $1.43''$ radius adopted by Schaefer & Pagnotta (2012). Within their new circle they found, from photometry obtained with the *HST*, no less than 21 stars with I-band magnitudes ranging from 26.9 to 20.51, which were still to be studied.

Litke et al. (2017) have also explored the central region of SNR 0509-67.5, adopting an explosion site that differs from that of Schaefer & Pagnotta (2012) by $1''.3$, and covering a circle of $3''$ radius around it (more than twice that adopted by these authors). By comparing the stars there with the post-impact explosion models of Pan, Ricker & Taam (2014), they conclude that no normal surviving companion is present.

The second SN Ia to be explored in the LMC was SNR 0519-69.0 (Edwards, Pagnotta & Schaefer 2012). The type of the remnant was assigned from the light echo of the SN and also from its X-ray emission. They used *HST* images with a limiting magnitude $V = 26.05$ mag. The circle explored, based on the same considerations as in the previous case, had a

radius of 4.7'' from the geometrical center of the SNR. It contained 27 main-sequence stars brighter than $V = 22.7$ mag, any of which might have been the companion, in the absence of further evidence. There were no post-main-sequence stars. The result thus pointed either to a supersoft X-ray source as the progenitor system of the SN or to its coming from the DD channel. This SNR has later been studied by Li et al. (2019) (see below).

Pagnotta & Schaefer (2015) observed two further SNRs of the SN Ia type in the LMC: SNR 0505-67.9 (also known as DEM L71) and SNR 0509-68.7 (or N103B). After locating their centers and tracing the corresponding 3σ circles, they have found possible candidates of all types: 121 stars in SNR 0505-67.9 (among them six red giants and one possible subgiant) and 8 stars in SNR 0509-68.7 (N103B). No channel nor type of progenitor system could either be confirmed or excluded by these observations.

More recently, Li et al. (2017) have also explored the SN Ia remnant N103B. The physical structures inside the SNR have been studied from $H\alpha$ and continuum images obtained with the *HST* and with high-dispersion spectra taken at the 4m and 1.5m telescopes of the Cerro Tololo Inter-American Observatory. After determining the explosion center, they have found, close to it, a star whose colors and luminosity are consistent with a $1 M_{\odot}$ subgiant companion concordant with a model by Podsiadlowski (2003). In this model, the star has a $0.2 M_{\odot}$ of envelope stripped and the rest is heated by the impact of the SN ejecta. No observations allowing to measure radial velocities, rotation or proper motions are yet available to either confirm or reject the proposed identification.

Li et al. (2019), in a new study of SN Ia remnants in the LMC, have examined three of them: 0519-69.0, 0505-67.9 (DEM L71), and 0548-70.4. New images of SNR 0519-69.0 and SNR 0548-70.4 have been obtained using the UVIS channel of the Wide Field Camera 3 (WFC3). SNR 0519-69.0, DEM L71 and SNR 0548-70.4 were observed with the Advanced CCD Imaging Spectrometer (ACIS) of the *Chandra* X-ray Observatory. Multi-Unit Spectroscopic

Explorer (MUSE) observations of SNR 0519-69.0 and DEM L71 were obtained with the Very Large Telescope (VLT) of the European Southern Observatory. Stellar parameters and radial velocities were derived from the spectra.

Li et al. (2019) have found a star in 0519-69.0 and another one in DEM L71 that move at high radial velocities, more than 2σ from the mean radial velocity of the populations explored. A photometrically peculiar star has been found in SNR 0548-70.4, but it might in fact be a background galaxy.

To search for possible surviving companions of the SNe Ia, Li et al. (2019) use two different methods. In the first one, the photometric measurements with the *HST*, of the stars around the center of the SNR, are used to construct color–magnitude diagrams (see Figure 17) and compare positions of the stars in the diagrams with the theoretical expectations of the post–impact evolution of MS and He–star companions. In the second method, they use spectroscopy with the Multi–Unit Spectroscopic Explorer (*MUSE*), at the ESO *VLT*, to find peculiar radial velocities as a mark of possible companions.

In the photometric approach, the calculations of the post–impact evolution in luminosity and effective temperature of surviving SN Ia companions of Pan, Ricker & Taam (2014) are used (as in Litke et al. 2017) to construct the theoretical color–magnitude diagrams that are compared with the observations. Only stars with $V < 22.7$ mag were considered. Any star falling on an evolutionary track whose age (that of the SNR) were consistent would be a companion candidate.

In the spectroscopic approach, the physical parameters and radial velocities of the stars within the search radius from the site of the explosion are determined. Here the magnitude limit is $V < 21.6$ mag. The photometric candidates brighter than this limit are then checked for large radial velocities as diagnostics of surviving companions.

SNR 0519-69.0 had previously been studied by Edwards, Pagnotta & Schaefer (2102), but the photometry of Li et al. (2019) is more complete, including the B , V , I and $H\alpha$ bands. Taking into account both the uncertainty on the center and the maximum runaway velocity of a possible He–star companion (the fastest moving case), Li et al. (2019) consider all stars with $V < 23.0$ within a search radius of $2''.7$ (corresponding to 0.65 pc at the distance of the LMC). That includes only eight stars. Their colour–magnitude diagrams are compared with the post–impact evolutionary tracks of MS and He stars. The authors conclude on the absence of viable candidates. Only five of these eight stars have $V < 21.6$ mag, and their stellar parameters and radial velocities have been determined. A radial velocity distribution has been obtained by including stars within a much larger distance from the explosion site. Only one star, moving at 182 ± 0 km s $^{-1}$, deviates more than 2.5σ from the mean velocity of the extended sample (264 km s $^{-1}$).

DEM L71 had been studied by Pagnotta & Schaefer (2015). The search radius is of $14''.5$, which corresponds to 3.7 pc. There is a total of 89 stars within that radius, with $V < 23.0$ mag. As in the case of SNR 0519-69.0, the theoretical evolutionary paths for surviving MS and He–star companions are overplotted on the observed color–magnitude diagrams. The comparison does not yield any candidate. There are 32 stars with $V < 21.6$ mag within the $14''.5$ radius, for which stellar parameters and radial velocities have been determined. When plotting the distribution of radial velocities, one star is at more than 2.5σ from the mean (213 ± 0 km s $^{-1}$ and 270 km s $^{-1}$, respectively).

SNR 0548-70.4 is explored for the first time by Li et al. (2019). Only the photometric approach has been possible. The search radius is of $40''.0$, corresponding to 10.0 pc. There are 973 stars with $V < 23.0$ mag there. Comparison of the color–magnitude diagrams with the theoretical evolutionary tracks does not reveal any promising candidate, but nevertheless one star has unusual photometric characteristics. Its colors are inconsistent

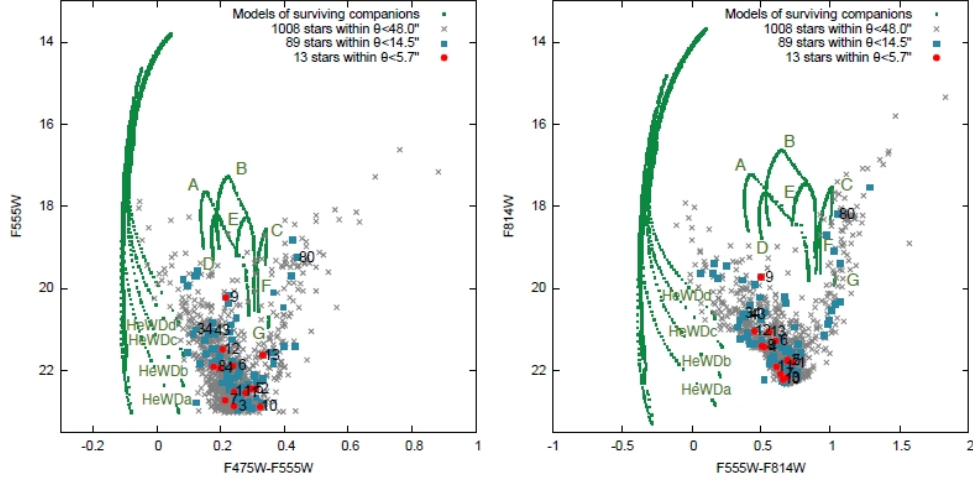


Fig. 17.— Left: V versus B–V colour–magnitude diagrams (CMD) of DEM L71. Right: I versus V–I CMD of DEM L71. Stars that are found within the runaway distances from the center for He–star and main–sequence (MS) surviving companions, are plotted as blue filled squares and red filled squares, respectively. Stars that are superposed on or near the remnant are plotted as grey crosses to illustrate the general background stellar population. The post–impacted evolutionary tracks are plotted as small green squares, and those of surviving He star and MS companions are to the left and above the MS, respectively. Different tracks of He stars and MS companions correspond to different companion masses in a range of 0.70 to 1.21 M_{\odot} and 1.17 to 1.88 M_{\odot} , respectively. The details of these He star and MS companions can be found in models from Pan, Ricker & Taam (2014). (Image and caption as in Li et al. 2019. Courtesy of W. Kerzendorf. @AAS. Reproduced with permission.)

with any spectral type. There is the possibility, however, that the object were not a star but a background galaxy. Infrared photometry, extending the observed spectral energy distribution, could discriminate between the two possibilities.

Summarizing, out of the five SN Ia remnants in the LMC that have already been explored to some extent, stars with radial velocities that are significantly higher than the mean for the corresponding population have been found in two of them (SNRs 0519-69.0 and DEM L71). A star with characteristics similar to those predicted by a model of the post-impact evolution of a surviving companion appears close to the center of SNR N103B, and a photometrically peculiar star in SNR 0548-70.4. Nothing has been found in SNR 0509-67.5. Further observations are needed to measure proper motions, rotational velocities and chemical abundances of the candidates found in SNRs 0519-69.0, DEM L71 and N103B (also the radial velocities, in the latter case), and to elucidate the true nature of the object in SNR 0548-70.4. Seven more, already identified remnants, remain to be explored.

4. Summary and conclusions

SNe Ia can, in principle, be produced through two different channels: the SD channel and the DD channel (the core-degenerate CD scenario, the merging of a WD with the electron-degenerate core of a red-giant star, being a variant of the DD channel). We still do not know, at present, in which proportions (including zero) does each channel contribute to the observed SNe Ia rate. Anyway, we can confidently discard that all SNe Ia would come from the classical SD channel.

In SNe Ia produced through the SD channel, the companion stars of the WDs that explode should, in general, survive the explosions and thus be detectable in deep enough surveys. In the case of recent SNe Ia, such companions cannot have travelled far from the site of the

explosion and must, therefore, still be in the central regions of the corresponding SNRs. Their clear absence there would be proof that the SN was produced through some variant of the DD channel.

In the last 15 years, several surveys have been made of SNRs of the Ia type, in our Galaxy and in the LMC, and others are in progress or have been planned. The remnants of the four “historical” SNe Ia (happened within the last 2,000 yr and for which we have records of their observations) have been explored in some depth, combining ground-based observations with others made with the *HST*. No clear-cut evidence of a surviving companion has been found in any of them, the case of a proposed companion in Tycho’s SNR remaining debated. In the case of SN 1604 (Kepler’s SN), the evidence excludes the SD scenario (Ruiz-Lapuente et al. 2018 suggest the CD scenario), and in that of SN 1006 a merging of two WDs origin is favored.

Up to now, five young SNe Ia remnants in the LMC have been explored to some extent, by means of the *HST* and of *Chandra* and other X-ray observatories, plus radio and other ground-based observations: SNR 0509–67.5, SNR 0519–69.0, SNR 0505–67.9 (or DEM L71), SNR 0509–68.7 (or N103B), and SNR 0548–70.4. In the first one, a DD origin (WD+WD merging) seems favored, but the searches might need to go deeper in magnitude to exclude the very faint companions. In the other four, there is one suggested companion (in SNR 0509–68.7/N103B), post-main-sequence companions are excluded in SNR 0519–69.0, and main-sequence companions in SNR 0505–67.9, and SN 0548–70.4 are being examined.

Thus far, the statistics (although still based on small numbers) seem to disfavor the SD channel. One source of uncertainty, however, is to which extent the spin-up/spin-down mechanism could be responsible for the failure to detect companions due to their faintness. If spin-down times are typically $t \approx 10^7$ yr and the absence of companions would persist in larger samples of remnants, the spin-up/spin-down mechanism might hardly be invoked as

an explanation any longer. In the case of SN 1006, the spin-up/spin-down may arguably be disfavoured by the observations of Kerzendorf et al. (2018b), that cover the presence of faint companions and found no evidence of dim ones, although this needs to be checked with hydrodynamical simulations of the supernova impact on very low mass stars.

Another point affecting the searches is the fact that the actual sites of the explosions may differ from the present centroids of the SNRs by a considerable angular distance, even in remnants that appear round. That should be taken into account in the searches, in addition to the angular distance a companion might have travelled in the time between the explosion and the observations.

Several already identified Galactic SNRs of the Ia type remain to be explored and a larger number in the LMC. So, the statistics can rapidly improve. In the future, not only new ground-based telescopes and the *HST* will be of use, but also the *JWST* could play an important role, as well as the astrometric data from the upcoming releases by the *Gaia* space mission. Some surviving companions must eventually be detected, unless the SD channel were not happening in nature.

5. Acknowledgements

The author would like to thank the coauthors of her papers related to the present review for sharing this exciting endeavour. She thanks the anonymous referee for his/her comments, that have been incorporated in the paper. Special thanks go to Wolfgang Kerzendorf for valuable comments, and suggestions on the draft, as well as for allowing the reproduction of various figures displayed in papers by him and his collaborators. Thanks go as well to the rest of authors of figures reproduced here with permission. P.R.-L. is supported by funds AYA2015-67854-P and PGC2018-095157-B-100 from the Ministry of Industry, Science

and Innovation of Spain and the FEDER funds.

REFERENCES

- Adibekyan, V.Zh., Sousa, S.G., Santos, N.C., et al. 2012, *A&A*, 545, A32
- Allen, G.E., Petre, R., & Gotthelf, E.V. 2001, *ApJ*, 558, 739
- Badenes, C, Bravo, E., Borkowski, K.J., & Domínguez, I. 2003, *ApJ*, 593, 358
- Badenes, C., Bravo, E., & Hughes, J.P. 2008, *ApJL*, 680, L33
- Bandiera, R. 1987, *ApJ*, 319, 885
- Bedin, L.R., Ruiz–Lapuente, P., González Hernández, J.I., et al. 2014 (B14), *MNRAS*, 439, 354
- Bensby, T., Feltzing, S., Lundström, I., & Ilyin, I. 2005, *A&A*, 433, 185
- Blair, W.P., Long, K.S., & Vancura, O. 1991, *ApJ*, 366, 484
- Bocchino, F., Vink, J., Favata, F., Maggio, A., & Scortino, S. 2000, *A&A*, 360, 671B
- Borkowski, K.J., Gwynne, P., Reynolds, S.P., et al. 2017, *ApJL*, 837, L7
- Busser, J.-U., Egger, R.J., & Aschenbach, B. 1995, *IAUC*, 6142
- Carlton, A.K., Borkowski, K.J., Reynolds, S.P., et al. 2011, *ApJL*, 737, L22
- Cassam–Chenaï, G., Decourchelle, A., Ballet, J., et al. 2004, *A&A*, 414, 545
- Caswell, J. L., Clark, D. H., Crawford, D. F., & Green, A. J. 1975, *Aust. J. Phys. Astrophys. Suppl.*, 37, 1
- Chakraborti, S., Childs, F., & Soderberg, A. 2016, *ApJ*, 819, 37
- Chiotellis, A., Schure, K.M., & Vink, J. 2012, *A&A*, 537, A139

- Clark, D.H., & Stephenson, F.R. 1977, *The Historical Supernovae* (Pergamon, New York)
- Cutri, R.M., et al. 2003, *VizieR Online Data Catalog* II/246
- Damiani, F., Prisinzano, L., Micela, G., et al. 2014, *A&A*, 566, A50
- Dave, P., Kashyap, R., Fisher, R., et al. 2017, *ApJ*, 841, 58
- Di Stefano, R., Voss, R., & Claeys, J.S.W. 2011, *ApJL*, 738, L1
- Di Stefano, R., & Kilic, M. 2012, *ApJ*, 759, 56
- Dubey, A., Fisher, R., Graziani, C., et al. 2008, in *Numerical Modeling of Space Plasma Flows*, ASP Conf. Ser., 385, 145
- Ecuvillon, A., Israelian, G., & Santos, N.C. 2004, *A&A*, 426, 619
- Ecuvillon, A., Israelian, G., & Santos, N.C. 2006, *A&A*, 445, 633
- Edwards, Z.I., Pagnotta, A., & Schaefer, B.E. 2012, *ApJL*, 747, L19
- Eggleton, P.P. 1973, *MNRAS*, 163, 279
- Eggleton, P.P. 1983, *ApJ*, 268, 368
- Fink, M., Röpke, F., Hillebrandt, W., et al. 2010, *A&A*, 514, 53
- Fryxell, B., Olson, K., Ricker, P., et al. 2000, *ApJS*, 131, 173
- García-Senz, D., Badenes, C., & Serichol, N. 2012, *ApJ*, 745, 75
- Giacani, E., Smith, M.J.S., Dubner, G., et al. 2009, *A&A*, 507, 841
- Giacani, E., Smith, M.J.S., Dubner, G., et al. 2011, *A&A*, 531, A138
- Gilli, G., Israelian, G., & Ecuvillon, A. 2006, *A&A*, 449, 723

- González Hernández, J.I., Ruiz–Lapuente, P., Filippenko, A.V., Foley, R.J., Gsl–Yam, A., & Simon, J.D. 2009 (GH09), *ApJ*, 691, 1
- González Hernández, J.I., Ruiz–Lapuente, P., Tabernero, H.M., et al. 2012, *Nature*, 489, 533
- Green, D.A. 2014, *Bull. Astr. Soc. India*, 00, 1.
- Greiner, J., & Egger, R. 1993, *IAU Circ.* 7709
- Greiner, J. & Egger, R., & Aschenbach, B. 1994, *A&A*, 286, L35
- Hachisu, I., Kato, M., & Nomoto, K. 1996, *ApJL*, 470, L97
- Hachisu, I., Kato, M., Nomoto, K., & Umeda, H. 1999, *ApJ*, 519, 314
- Hachisu, I., Kato, M., & Nomoto, K. 2008, 679, 1390
- Han, Z. 2008, *ApJL*, 677, L109
- Harrus, I.M., Sloane, P.O., Smith, R.K., & Hughes, J.P. 2001, *ApJ*, 552, 614
- Hendrick, S.P., Borkowski, K.J., & Reynolds, S.P. 2003, *ApJ*, 593, 370
- Hillebrandt, W., & Niemeyer, J.C. 2000, *ARA&A*, 38, 191
- Hillebrandt, W., Kromer, M., Röpke, F.K., & Ruiter, A.J. 2013, *FrPhy*, 8, 116
- Hovey, L. 2016, PhD Thesis, Stat Univ. New Jersey
- Hovey, L, Hughes, J.P., & Eriksen, K. 2015, *ApJ*, 809, 119
- Hovey, L., Hughes, J.P., & Eriksen, K. 2016, in *Supernova Remnants: An Odyssey in Space after Stellar Death*, 38
- Hughes, J.P., Hayashi, I.H., & Koyama, K. 1998, *ApJ*, 505, 732

- Iben, I., Jr. 1984, & Tutukov, A.V. 1984, *ApJS*, 54, 335
- Ihara, Y., Ozaki, J., Doi, M., et al. 2007, *PASJ*, 59, 811
- Jiang, J.-A., Doi, M., Maeda, K., et al. 2017, *Nature*, 550, 80
- Johansson, J., Woods, T.E., Gilfanov, M., Sarzi, M., Chen, Y.-M., & Oh, K. 2014, *MNRAS*, 442, 1079
- Johansson, J., Woods, T.E., Gilfanov, M., et al. 2016, *MNRAS*, 461, 4505
- Justham, S. 2011, *ApJL*, 730, L34
- Kamitsukasa, F., Koyama, K., Nakajima, H., et al. 2016, *PASJ*, 68, S7
- Kashi, A., & Soker, N. 2011, *MNRAS*, 417, 1466
- Katsuda, S., Mori, K., Maeda, K., et al. 2015, *ApJ*, 808, 49
- Kerzendorf, W.E., Schmidt, B.P., Asplund, M., et al. 2009, *ApJ*, 701, 1665
- Kerzendorf, W.E., Schmidt, B.P., Laird, J.B., et al. 2012, *ApJ*, 759, 7
- Kerzendorf, W.E., Yong, D., Schmidt, B.P., et al. 2013 (K13), *ApJ*, 774, 99
- Kerzendorf, W.E., Childress, M., Scharwächter, J., Do, T., & Schmidt, B.P. 2014, *ApJ*, 782, 27
- Kerzendorf, W.E., Long, K.S., Winkler, P.F., & Do, T. 2018a, *MNRAS*, 479, 5696
- Kerzendorf, W.E., Strampelli, G., Shen, K.J., et al. 2018b, *MNRAS*, 479, 192
- Kinugasa, K., Torii, K., Tsunemi, H., et al. 1998, *PASJ*, 50, 249
- Krause, O., Tanaka, M., Usuda, T., et al. 2008, *Nature*, 456, 617

- Leahy, D.A., & Ranasinghe, S. 2016, *ApJ*, 817, 74
- Leonard, D.C. 2007, *ApJ*, 670, 1275
- Li, C.-J., Chu, Y.-H., Gruendl, R.A., et al. 2017, *ApJ*, 836, 8
- Li, C.-J., Kerzendorf, W.E., Chu, Y.-H., et al. 2019, *ApJ*, 886, 99
- Litke, K.C., Chu, Y.-H., Holmes, A., et al. 2017, *ApJ*, 837, 111
- Liu, Z.-W., Pakmor, R., Röpke, F., et al. 2013, *A&A*, 554, 109
- Livio, M. 2013, in *Binary Paths to Type Ia Supernovae Explosions*, IAU Symposium 281, 303
- Livio, M., & Riess, A.G., 2003, *ApJL*, 594, L93
- Long, K. S., Helfand, D. J., & Grabelsky, D. A. 1981, *ApJ*, 248, 925
- Lopez, L. A., Ramirez-Ruiz, E., Huppenkothen, D., Badenes, C., & Pooley, D. A. 2011, *ApJ*, 732, 114
- Lu, F.J., Wang, Q.D., Ge, M.Y., et al. 2011, *ApJ*, 732, 11
- Maeda, K., Benetti, S., Stritzinger, M., et al. 2010, *Nature*, 466, 82
- Maoz, D., Mannucci, F., & Nelemans, G. 2014, *ARA&A*, 52, 107
- Marietta, E., Burrows, A., & Fryxell, B. 2000, *ApJS*, 128, 615
- Martínez-Rodríguez, H., Badenes, C., Yamaguchi, H., et al. 2017, *ApJ*, 843, 35
- McEntaffer, R.L., Grieves, N., DeRoo, C., & Brantseg, T. 2013, *ApJ*, 774, 120
- Meng, X., & Podsiadlowski, P. 2013, *ApJL*, 778, L35

- Meng, X., & Podsiadlowski, P. 2017, MNRAS, 469, 4763
- Meng, X., & Li, J. 2019, MNRAS, 482, 5651
- Neves V., Santos N. C., Sousa S. G., et al. 2009, A&A, 497, 563
- Nomoto, K. 1982, ApJ, 253, 798
- Nomoto, K. & Leung, S.-C. 2017, in *Handbook of Supernovae* (Springer Intl. Publ.), 1275
- Ostriker, J.P., & Bodenheimer, P. 1968, ApJ, 151, 1
- Pagnotta, A., & Schaefer, B.E. 2015, ApJ, 799, 101
- Pakmor, R., Röpke, F.K., Weiss, A., & Hillebrandt, W. 2008, A&A, 489, 943
- Pan, K.C., Ricker, P.M., & Taam, R.E. 2012a, ApJ, 750, 151
- Pan, K.C., Ricker, P.M., & Taam, R.E. 2012b, ApJ, 760, 21
- Pan, K.-C., Ricker, P.M., & Taam, R.E. 2014, ApJ, 792, 71
- Park, S., Slane, P., Hughes, J., et al. 2007, ApJ, 665, 1173
- Park, A., & Post, S. 2016, in *Supernova Remnants: An Odyssey in Space after Stellar Death*, 76
- Paunzen, E. 2004, in *The A–Star Puzzle*, IAU Symp. 224 (Cambridge, UK: Cambridge Univ. Press), 443
- Paxton, B., Bildsten, L., Dotter, A., et al. 2011, ApJS, 192, 3
- Perlmutter, S., Aldering, G., Goldhaber, G., et al. 1999, ApJ, 517, 565
- Petruk, O. 1999, A&A, 346, 961

- Podsiadlowski, P. 2003, arXiv:0303.660
- Post, S., Park, S., Badenes, C., et al. 2014, ApJL, 792, L20
- Rakowski, C.E., Badenes, C., Gaensler, .M., et al. 2006, ApJ, 646, 982
- Rest, A., Suntzeff, N. B., Olsen, K., et al. 2005, Nature, 438, 1132
- Rest, A., Matheson, T., Blondin, S., et al. 2008, ApJ, 680, 1137
- Reynolds, S.P., Borkowski, K.J., Green, D.A., et al. 2008, ApJL, 680, L41
- Reynoso, S.P., Borkowski, K.J., Hwang, U., et al. 2007, ApJL, 66, L135
- Riess, A.G., Filippenko, A.V., Challis, P., et al. 1998, AJ, 116, 1009
- Robin, A.C., Reyl  , C., Derri  re, S., & Picaud, S. 2003, A&A, 409, 523
- Rosado, M., Ambrocio–Cruz, P., Le Coarer, E., & Marcelin, M. 1996, A&A, 315, 243
- Ruiz-Lapuente, P. 1997, Science, 276, 1813
- Ruiz–Lapuente, P. 2004, ApJ, 612, 357
- Ruiz–Lapuente, P., Comer  n, F., M  ndez, J., et al. 2004 (RL04), Nature, 431, 1069
- Ruiz–Lapuente, P. 2014, NewAR, 62, 15
- Ruiz–Lapuente, P. 2017, ApJ, 842, 112
- Ruiz–Lapuente, P., Damiani, F., Bedin, L., et al. 2018, ApJ, 862, 124
- Ruiz–Lapuente, P., Gonz  lez Hern  ndez, J.I., Mor, R., et al. 2019, ApJ, 870, 135
- Sankrit, R., Raymond, J.C., Blair, W.P., et al. 2016, ApJ, 817, 36
- Sano, H., Yamane, Y., Tokuda, K., et al. 2018, ApJ, 867, 7

- Sato, T., & Hughes, J.P. 2017, *ApJ*, 845, 167
- Schaefer, B.E., & Pagnotta, A. 2012, *Nature*, 481, 164
- Schlaafly, E.P., & Finkbeiner, D.P. 2011, *ApJ*, 737, 103
- Sezer, A., & Gök, F. 2014, *ApJ*, 790, 81
- Shappee, B.J., Kochanek, C.S., & Stanek, K.Z. 2013, *ApJ*, 765, 150
- Shen, K.J., & Schwab, J. 2017, *ApJ*, 834, 180
- Shen, K.J., Boubert, D., Gänsicke, B.T., et al. 2018, *ApJ*, 865, 15
- Sim, S.A., Fink, M., Kromer, M., et al. 2012, *MNRAS*, 420, 3003
- Soker, N. 2013, in *Binary Paths to Type Ia Supernovae Explosions*, IAU Symposium 281, 72
- Soker, N., García-Berro, E. & Althaus, L.G. 2014, *MNRAS*, 437, L66
- Soker, N. 2019, *SCPMA*, 62, 119501
- Sollerman, J., Ghavamian, P., Lundquist, P., & Smith, R.C. 2003, *A&A*, 407, 249
- Springel, V., Yoshida, N., & White, S.D.M. 2001, *New Astron.*, 6, 79
- Springel, V. 2005, *MNRAS*, 364, 1105
- Stephenson, F.R. 2010, *Astron. Geophys.*, 51, 5.27
- Tsebrenko, D., & Soker, N. 2013, *MNRAS*, 435, 320
- Tremblay P.-E., Ludwig H.-G., Steffen M., Bergeron P., & Freytag B., 2011, *A&A*, 531, L19
- Tuohy, J.R., Dopita, M.A., Mathewson, D.S., Long, K.S., & Helfand, D.J. 1982, *ApJ*, 261, 473

- Vink, J. 2008, *ApJ*, 689, 231
- Vink, J. 2017, in *Handbook of Supernovae*, ed. A. Absalti & P. Murdin (Cham: Springer), 139
- Wang, B., & Han, Z. 2012, *NewAR*, 56, 122
- Warren, J. S., & Hughes, J. P. 2004, *ApJ*, 608, 261
- Webbink, R.F. 1984, *ApJ*, 277, 355
- Wheeler, J.C., McKee, C.F., & Lecar, M. 1974, *ApJL*, 192, L71
- Wheeler, J.C., Lecar, M., & McKee, C.F. 1975, *ApJ*, 200, 145 x
- Whelan, J., & Iben, I. 1973, *ApJ*, 186, 1007
- Williams, B.J., Blair, W.P., Blondin, J.M., et al. 2011, *ApJ*, 741, 96
- Williams, B.J., Borkowski, K.J., Ghavamian, P., et al. 2013, *ApJ*, 770, 129
- Williams, B.J., Chomiuk, L., Hewitt, J.W., et al. 2016, *ApJ*, 823, L32
- Winkler, P.F., Gupta, G., & Long, K.S. 2003, *ApJ*, 585, 324
- Winkler, P.F., Long, K.S., Hamilton, A.J.S., & Fesen, R.A. 2005, *ApJ*, 624, 189
- Winkler, P.F., Williams, B.J., Reynolds, S.P., et al. 2014, *ApJ*, 781, 65
- Woods, T.E., & Gilfanov, M. 2013, *MNRAS*, 432, 1640
- Woods, T.E., & Gilfanov, M. 2014, *MNRAS*, 439, 2351
- Woods, T. E., Ghavamian, P., Badenes, C., & Gilfanov, M. 2017, *Nature Astronomy*, 1, 800
- Woods, T.E., Ghavamian, P., Badenes, C., & Gilfanov, M. 2018, *ApJ*, 863, 120

- Xue, Z., & Schaefer, B.E. 2015, ApJ, 809, 183
- Yamaguchi, H., Tanaka, M., Maeda, K., et al. 2012, ApJ, 749, 137
- Yamaguchi, H., Badenes, C., Petre, R., et al. 2014, ApJL, 785, L27
- Yamaguchi, H., Badenes, C., Foster, A.R., et al. 2015, ApJL, 801, L31
- Yoon, S., & Langer, N. 2004, A&A, 419, 623
- Yoon, S., & Langer, N. 2005, A&A, 435, 967
- Zhou, P., Chen, Y., Zhang, Z.-Y. 2016, ApJ, 826, 34